Published in final edited form as:
Cereb Cortex. 2008 May ; 18(5): 1058–1078. doi:10.1093/cercor/bhm137.

Lack of Orientation and Direction Selectivity in a Subgroup of Fast-Spiking Inhibitory Interneurons: Cellular and Synaptic Mechanisms and Comparison with Other Electrophysiological Cell Types

Lionel G. Nowak[1], **Maria V. Sanchez-Vives**[2], and **David A. McCormick**[3]

[1] CerCo, Université Toulouse 3, CNRS, Faculté de Médecine de Rangueil, 31062 Toulouse Cedex 9, France

[2] Instituto de Neurociencias de Alicante, Universidad Miguel Hernandez-CSIC, Apartado 18, 03550 San Juan de Alicante, Spain

[3] Department of Neurobiology and the Kavli Institute for Neuroscience, Yale University School of Medicine, New Haven, Connecticut 06510, USA

Abstract

Neurons in cat area 17 can be grouped in 4 different electrophysiological cell classes (regular spiking, intrinsically bursting, chattering, and fast spiking [FS]). However, little is known of the functional properties of these different cell classes. Here we compared orientation and direction selectivity between these cell classes in cat area 17 and found that a subset of FS inhibitory neurons, usually with complex receptive fields, exhibited little selectivity in comparison with other cell types. Differences in occurrence and amplitude of gamma-range membrane fluctuations, as well as in numbers of action potentials in response to optimal visual stimuli, did not parallel differences observed for orientation and direction selectivity. Instead, differences in selectivity resulted mostly from differences in tuning of the membrane potential responses, although variations in spike threshold also contributed: weakly selective FS neurons exhibited both a lower spike threshold and more broadly tuned membrane potential responses in comparison with the other cell classes. Our results are consistent with the hypothesis that a subgroup of FS neurons receives connections and possesses intrinsic properties allowing the generation of weakly selective responses. The existence of weakly selective inhibitory neurons is consistent with orientation selectivity models that rely on broadly tuned inhibition.

Keywords

direction selectivity; 40 Hz oscillation; inhibition; intracellular recording; orientation selectivity; spike threshold

Address correspondence to Dr David A. McCormick, Department of Neurobiology and the Kavli Institute for Neuroscience, Yale University School of Medicine, 333 Cedar Street, New Haven, Connecticut 06510, USA. david.mccormick@yale.edu.

Conflict of Interest: None declared.

Supplementary Material
Supplementary material can be found at http://www.cercor.oxfordjournals.org/.

Introduction

Computations performed by sensory systems depend on the way synaptic inputs are integrated and on how they are transformed into spiking outputs. This transformation in turn depends heavily on neuronal intrinsic membrane properties. In the cerebral cortex, neuronal membrane properties are far from homogeneous and, accordingly, different electrophysiological cell types have been distinguished (Calvin and Sypert 1976; Cauli et al. 1997; Connors et al. 1982; Gibson et al. 1999; Gray and McCormick 1996; Gupta et al. 2000; Kawaguchi 1995; McCormick et al. 1985; Mountcastle et al. 1969). In cat area 17, intracellular recording in vivo and quantitative analysis of firing properties have revealed 4 major electrophysiological cell classes: regular spiking (RS), fast spiking (FS), intrinsically bursting (IB), and chattering (CH) cells (Nowak et al. 2003). These cell types are distinguished by the generation of bursts with low (IB) or high (CH) intraburst frequency (IBF), brief duration action potentials (FS and CH), a steep frequency versus injected current relation (FS), or the presence of spike frequency adaptation (RS). Morphologically, FS cells are often basket or chandelier γ-aminobutyric acidergic (GABAergic) cells (Angulo et al. 1999; Azouz et al. 1997; Hirsch 1995; Kawaguchi 1995; Krimer et al. 2005; McCormick et al. 1985), whereas IB, CH, and RS cells appear to be excitatory neurons in most cases: spiny stellate cells in layer 4 and pyramidal cells in all layers (e.g., Chagnac-Amitai et al. 1990; Gray and McCormick 1996; Larkman and Mason 1990; McCormick et al. 1985; Nowak et al. 2003).

Given the differences in electrophysiological properties, the distinct cell classes mentioned above are likely to perform different transformations on their afferent inputs. However, in order to gain a better understanding of the role played by these different cell types, it is also necessary to examine their “functional” properties, such as the features of sensory information that these neurons transmit. The functional properties that we examined here are orientation and direction selectivity.

Both orientation and direction selectivity are first expressed in area 17 (Hubel and Wiesel 1962). Although these properties have been characterized more than 50 years ago, experimental and theoretical studies have somehow failed to yield a unified view of the mechanisms that generate them (reviewed in Ferster and Miller 2000; Martin 1988; Shapley et al. 2003; Sompolinsky and Shapley 1997; Vidyasagar et al. 1996). However, it is generally accepted that inhibition plays an important role in the sharpening of orientation and direction selectivity. For that reason, we were particularly interested in examining these properties in FS cells, which represent a subtype of inhibitory interneuron. Suspected interneurons in rabbit cortex have been reported to lack orientation and direction selectivity (Swadlow and Weyand 1987; Swadlow 1988), but the picture is less clear in cat area 17 where studies usually reported inhibitory interneurons to be orientation selective (Ahmed et al. 1997; Gabbott et al. 1988; Kisvarday et al. 1987; Martin et al. 1983, 1989; Azouz et al. 1997). However, one study demonstrated that a significant proportion of layer 4 inhibitory neurons lack orientation selectivity (Hirsch et al. 2003).

We found that, on average, FS cells in cat V1 are less selective for direction and orientation than cells in all the other 3 classes. Using cluster analysis, we further revealed the existence of a subgroup of cells characterized by very weak orientation and direction selectivity; this cluster contained mostly FS cells. We further examined which mechanisms could account for this weak orientation and direction selectivity in these cells and found that it results at least in part from the lack of tuning in their synaptic barrages as well as a lower than average spike threshold. Preliminary results have been presented in abstract form (Nowak et al. 2005a).

Methods

Surgical Protocol

The protocol for cat preparation, electrophysiological recordings, and data acquisition have been detailed in Sanchez-Vives et al. (2000) and is briefly summarized here. Experiments were performed on adult cats weighing 2.5–3.5 kg. Anesthesia was induced with ketamine hydrochloride (12–15 mg/kg) and xylazine (1 mg/kg) injected intramuscularly. Atropine (0.05 mg/kg) was injected subcutaneously to reduce secretions. Wires were inserted through the skin for electrocardiogram recording. An endotracheal tube was inserted to allow artificial ventilation, and a forelimb vein was cannulated for intravenous perfusion. Once the cat was set in the stereotaxic frame, it was artificially ventilated with nitrous oxide and oxygen (2:1) with halothane (1.5% during surgery) or with oxygen with isoflurane (2.5% during surgery). Epidural electroencephalographic (EEG) recording was performed through wires inserted over the frontal cortex. To minimize movements resulting from respiration and heartbeat, a cisternal drainage and a bilateral pneumothorax were performed and the animal was suspended by the rib cage to the stereotaxic frame. A 3- to 4-mm-wide craniotomy was made to gain access to area 17. Following surgery, the animal was paralyzed with Pavulon (0.3 mg/kg for induction followed by a continuous perfusion of 0.3 mg/kg/h) or Norcuron (0.15 mg/kg for induction followed by a continuous perfusion of 0.1 mg/kg/h). The nictitating membranes were retracted using ophthalmic phenylephrine and the pupils dilated and accommodation paralyzed with ophthalmic atropine. The area centralis and optic discs were localized by back projection. Corrective, gas permeable contact lenses were used to protect and focus the eyes onto a computer monitor at 114 cm. During recording, anesthesia was maintained with 0.4–1% halothane in nitrous oxide-oxygen (2:1) or with 0.5–2% isoflurane in oxygen. The heart rate, expiratory CO_2 concentration, rectal temperature, and blood O_2 concentration were monitored throughout the experiment and maintained at 150–180 bpm, 3–4%, 37–38 °C, and >95%, respectively. The EEG and the absence of reaction to noxious stimuli were regularly checked. This protocol was approved by the Yale University Institutional Animal Care and Use Committees and conforms to the guidelines recommended in “Preparation and Maintenance of Higher Mammals During Neuroscience Experiments,” NIH publication No. 91–3207.

Intracellular Recording Procedure

Intracellular recordings were made with sharp micropipettes pulled on a P-80 micropipette puller (Sutter Instruments, Novato, CA) from medium-walled glass capillaries (1BF100, Sarasota, FL). The micropipettes were filled with potassium acetate (2 M). In some experiments, they also contained biocytin (2%; Molecular Probes, Eugene, OR). The micropipettes were beveled (Sutter Instruments beveller) to a final resistance of 50–100 MΩ. To prevent drying and to minimize brain movements during recording, exposed cortex was covered with warm agar (4% in artificial cerebrospinal fluid). Intracellular data were taken into account only if the membrane potential was more negative than −55 mV at rest, the input resistance larger than 20 MΩ, and the neuron able to discharge trains of action potentials during the whole duration of 300 ms depolarizing current pulses.

Cell Type Identification

The intracellularly recorded cells (n = 111) were classified according to their electrophysiological properties as RS, FS, IB, or CH. Part of the sample (n = 35 cells) corresponds to cells that have been used in a previous study (Nowak et al. 2003) to establish quantitative criteria for identification of electrophysiological cell classes. The criteria set in that study were used to perform the electrophysiological identification of the remaining cells (n = 76). For most of these cells (n = 55/76), responses to series of depolarizing current pulses (120–300 ms duration, intensity increment of 0.1 nA, and maximal intensity 1 nA)

were used to induce repetitive firing. Examples of responses to current pulses are presented in Figure 1 for each cell type. First, we examined the distribution of the log values of the interspike intervals (ISIs) for the spikes induced by the current pulses. Bimodal distribution of log(ISIs) characterizes neurons that generate bursts of action potentials (Fig. 1*C*,*F*). In burst-generating neurons, the intraburst frequency (IBF) allowed the identification of IB (IBF < 350 Hz) and CH (IBF > 425 Hz) cells. These differences in IBF are linked to action potentials duration that tend to be longer in IB cells (Fig. 1*B*) compared with CH cells (Fig. 1*E*). Cells with IBF between 350 and 425 Hz were further identified according to their burst inactivation properties. Typically, in IB cells (Fig. 1*A*), bursts discharge tends to inactivate as a function of time elapsed since the beginning of the current injection, whereas CH cells discharge action potential bursts for the whole length of the current injection (Fig. 1*D*). Cells that did not generate action potential bursts are identified by unimodal log(ISIs) distribution (Fig. 1*I*,*L*). In these cells, the action potential width was first used to differentiate between RS and FS neurons. RS cells usually (but not always) show broad action potentials (Fig. 1*H*) and spike frequency adaptation (Fig. 1*G*). Cells with spike width at half height (measured from threshold) >0.5 ms unambiguously correspond to RS cells. However, when spike width was <0.5 ms, the strength of firing rate adaptation has to be examined in order to differentiate between thin-spike RS cells and FS cells. FS cells are characterized by both thin action potentials (Fig. 1*K*) and by firing rates that adapt mildly or not at all with 300ms pulse duration, (Fig. 1*J*).

Not all cells received a series of current pulses; in some experiments, priority was given to visual responses properties and current pulses were given after completion of visual stimulation protocols. Not all cells were kept up to that point. For these cells (n = 21/76), we relied on the IBF and spike width obtained in response to visual stimulation (IBF and spike width obtained with visual stimulation are very similar to those obtained with current injections—Gray and McCormick 1996; Cardin et al. 2005). Burst generating cells with IBF between 350 and 425 Hz and nonbursting cells with spike width <0.5 ms could not be classified in these instances.

Spike threshold was determined using a spike-triggered average of the membrane potential. Threshold was taken as the time of rapid inflection of the membrane potential. Baseline was taken as the flattened portion of the average at a large temporal distance (>1–2 s, corresponding to spontaneous activity period) from the triggering spike. Another way to determine threshold has been proposed that relies on the analysis of the relationship between spike rate and membrane potential (Anderson 2000; Hansel and van Vreeswijk 2002; Miller and Troyer 2002; Priebe et al. 2004). However, this measure might actually correspond to another kind of threshold, to which we might refer to as a “firing rate threshold” rather than as a “spike threshold.” The nonlinearity that appears in this relationship is likely due to the presence of noise in the membrane potential. In particular, this means that, all parameters being kept constant, “firing rate threshold” will decrease with increase in noise. In this situation, threshold is not dictated by the intrinsic membrane properties of the cells anymore but by the (external) presence of synaptic noise.

Identification of FS Cells

Only a fraction of the cells we recorded from have been labeled and their morphology examined. The main conclusions of this study therefore rest on the identification of a subclass of inhibitory neurons—the FS cells—by their electrophysiological properties (Nowak et al. 2003). This approach seems to be well grounded, given the large number of studies (McCormick et al. 1985; Hirsch 1995; Kawaguchi 1995; Azouz et al. 1997; Angulo et al. 1999; Krimer et al. 2005) that have demonstrated that FS cells always display the morphological features of inhibitory neurons (e.g., basket and chandelier cells). However, the converse is not true: morphologically identified inhibitory neurons do not all display FS

electrophysiological properties. Indeed, in vitro studies (Foehring et al. 1991; Deuchars and Thomson 1995; Kawaguchi 1995; Cauli et al. 1997; Gupta et al. 2000; Krimer et al. 2005) also identified various types of inhibitory neurons, whose firing properties are different from those of FS cells and may be relatively close to those of IB, CH, or RS cells. However, even if we had recorded from these non-FS inhibitory neurons and had classified them in the IB, CH, or RS classes, in our sample, they would have been largely outnumbered by excitatory IB, CH, and RS cells (Nowak et al. 2003). In the absence of a definite morphological identification, orientation and direction selectivity of non-FS inhibitory neurons remain to be established.

Visual Stimulation

The receptive field's location, length, and velocity preference were first determined with a handheld projector. Subsequently, visual stimuli, generated using a VSG-Series 3 system (Cambridge Research Systems, Cambridge, UK), were presented under computer control on a 19-inch color monitor (80 Hz noninterlaced refresh; 1024 × 768 resolution).

In all cases, orientation selectivity was determined using drifting bars as a stimulus. The bars were either black on a light gray background or white on a dark gray background (Michelson contrast: 80%). Bars were presented with 8 different orientations, in steps of 22.5°, each time with 2 motion directions, making a total of 16 different stimuli. The 16 stimuli were presented sequentially. The bar width and bar height were kept constant in all experiments, at 0.5° and 6°, respectively. The drift velocity was between 4 and 8 deg/s. A 1 s duration, pause was inserted between each stimulus presentation.

Simple/Complex Cell Classification

Simple versus complex cell classification relied on the use of quantitative analysis based either on the response to drifting sinewave gratings, on the response to drifting light and dark edges, or on 1-dimensional receptive field mapping using flashing bars. Our simple/complex cell classification thus often relied on time-consuming visual stimulation paradigms; several cells (14/111) have been lost before completion of these tests, and their RF types could not be determined.

When using sinewave gratings (n = 65/97 cells), the spiking response to the preferred spatial frequency was Fourier analyzed and the F0 (mean response) and F1 (response amplitude at the frequency of the grating drift) components extracted. The ratio of F1/F0, or "relative modulation" index (Skottun et al. 1991), was then used to classify cells as simple or complex. In our data, the distribution of the relative modulation indices was bimodal, with a gap at 1.0. Based on this distribution, we considered cells as simple when the relative modulation index was >1 and complex when it was <1 (Skottun et al. 1991).

Edge responses (n = 10/97 cells) were generated by using wide drifting light and dark bars presented in the optimal orientation. Peristimulus time histograms (PSTHs) revealed responses to light-to-dark and dark-to-light edges that showed little or no spatial overlap in simple cells, whereas they did overlap extensively in the complex cells (Schiller et al. 1976a).

In the RF mapping procedure (n = 22/97 cells), optimally oriented bright and dark bars were flashed at 20 Hz across the RF in 16 randomly varying spatial positions. Space-time RF maps were constructed for the spiking responses (McLean and Palmer 1989; Palmer and Davis 1981; procedure detailed in Nowak et al. 2005b). The simple/complex cell identification relied on the amount of spatial overlap for bright and dark bar spiking responses: an overlap index for bright excitatory subregions (~on subregions) and dark excitatory subregions (~off subregions) was calculated and was found to be bimodal, as

found in other studies (Heggelund 1986; Martinez et al. 2005; Mata and Ringach 2005). Cells showing a good segregation of their bright and dark bar response regions corresponded to simple cells, whereas complex cells typically showed a strong spatial overlap for these subregions.

Data Analysis

For the quantitative analysis of orientation selectivity, we first computed PSTHs of the spiking responses and averages of the membrane potential for each of the 16 stimuli. The mean and standard deviation (SD) of the spontaneous activity level were calculated across all orientations. A time window (0.6–1.7 s wide) was set around the visually evoked synaptic response and the mean amplitude extracted for each orientation. The mean response amplitude for the spiking response was calculated over the same time window as the one used for calculating the mean synaptic response. Because synaptic responses lasted longer than spiking responses, the use of this single time window would have resulted in firing rates lower than what they would have been, had we centered the window strictly on the spiking responses. Furthermore, the crossing point of the drifting bars trajectory was not always exactly centered on the receptive fields, such that the responses could start at different times for the different orientations and directions. The time window used to delineate the visual response therefore necessarily included some time during which the neuron was not yet responding to the stimulus. For this reason, we used the number of spikes per stimulus (firing rate multiplied by window width) as a measure of spiking response strength rather than mean firing rates.

All subsequent analyses were done after removal of the spontaneous activity level. Synaptic responses amplitude corresponds to the mean amplitude of the membrane potential above (or below) resting membrane potential, and the mean number of spikes per stimulus are the mean above (or below) spontaneous activity level.

Spiking responses were considered to be significant only if at least one of the 16 responses was 3 times larger than the SD calculated for the spontaneous activity. Synaptic responses were taken into account only in cells that showed significant spiking response. Synaptic responses were considered significant if at least one of the response was at least 2 SDs larger than the spontaneous activity (in 74% of the cases, it was actually larger than 3 SD).

Parametric Analysis

Quantification of orientation tuning was achieved by fitting the Von Mises equation (Ringach et al. 2003; Swindale 1998) to the data. The equation has been modified to fit pairs of peaks over 360° instead of a single peak over 180°. It was implemented in Origin® software nonlinear fitter. A chi-square minimization procedure was used to optimize the fit. The equation for the fit was

$$y=y_0+A_1\exp\{k[\cos(\theta-\theta_c+\pi)-1]\}+A_2\exp\{k[\cos(\theta-\theta_c+\pi)-1]\},$$

where y_0 corresponds to a nonoriented component of the response (note that it does not correspond to spontaneous activity that was removed prior to fitting). θ is the orientation (in radians). A_1 corresponds to the amplitude of the response (in mV or in spikes/s) at the preferred orientation, θ_c, and A_2 to the amplitude of the response for the antipreferred direction. k is a width factor from which the half width at half height (HWHH, in deg) of the tuning function can be calculated as

$$\mathrm{HWHH}=(180/\pi)^{*}\arccos[(1\,n0,5+k)/k)].$$

We also calculated a "relative unselective response amplitude" (RURA), which corresponds to the ratio $y_0/(y_0 + A_1)$, expressed as a percentage. In cells that are well tuned, y_0 (the nonoriented component) is negligible and the ratio is close to 0. In cells that show no orientation and no direction selectivity, A_1 (the amplitude at the preferred orientation) would be negligible and the ratio would be close to 100%. In cells that show firing rates lower than spontaneous activity or membrane potential hyperpolarization below resting membrane potential for nonprefered orientation, the ratio takes a negative value.

Note that the RURA and HWHH do not provide equivalent measures of selectivity (cf., Fig. 7*B*). Cells may display a large unselective response amplitude topped by a sharply tuned response. Conversely, cells may show large HWHH but nevertheless relative unselective response close to 0%.

The third variable we used to characterize cells tuning is the "direction nonselectivity index" (DnSI), calculated as $100[(y_0 + A_2)/(y_0 + A_1)]$. DnSI is 100% in cells that are not direction selective, it is 0% in cells that respond to only one stimulus direction, and it is 50% for cells in which the response in the preferred direction is twice larger than the response in the antipreferred direction.

In some cases (9 spiking and 9 synaptic tuning curves), the response at 90° from the preferred orientation appeared larger than the minimum response, resulting in "secondary peaks" in the orientation tuning data (orthogonal secondary peaks have been described previously in several studies: De Valois et al. 1982; Ringach et al. 2003). These secondary peaks were taken into account by adding the following terms to the equation:

$$A_o\exp\{k_o[\cos(\theta-\theta_c)+(\pi/2)]-1\}+A_o\exp\{k_o\cos[(\theta-\theta_c)-(\pi/2)]-1\},$$

where A_0 and k_0 represent the amplitude and width of the orthogonal secondary peaks. These additional terms were added only for improving the fitting quality and are not further discussed here.

In some cases, especially when the tuning was broad, the fit did not stabilize despite the use of >100 iterations. Our strategy in these cases was to fit the data using pairs of Gaussian curves (constrained to have the same width), which never failed to stabilize, and to use the y_0 value obtained in these fits as a fixed parameter for the Von Mises fits.

Fits quality was given by the r^2 values. Data were included for further analysis only if the r^2 of fit was larger than 0.5 (except for spike responses in 2 unselective FS cells). Median r^2 value for spiking response was 0.919 (n = 111 cells). That for synaptic responses was 0.762 (n = 68 fitted cells).

Sample size differs for spiking and synaptic responses for several reasons. First of all, membrane potential data acquired in 7 cells in the earliest experiments with a different computer system have become unavailable, such that only the spiking responses could be analyzed for these cells. In addition, 9 cells were not considered because their synaptic responses did not reach significance level (although significant spiking responses were obtained in these instances). Among cells that showed significant responses, the postsynaptic response amplitude at 90° from the preferred orientation for spiking response represented >80% of the depolarization obtained for the preferred orientation in 6 cells. The

postsynaptic response in these cells was therefore considered as nonorientation selective and was given a HWHH of 90°. And finally, 21 cells showed significant synaptic responses, an orthogonal response amplitude <80% of the preferred response amplitude, but were not included in the sample because they could not be fit correctly (r^2 of fit < 0.5). These 21 cells were excluded not because the Von Mises model we used was inadequate for fitting them but because of the large amount of synaptic noise present in the membrane potential data; using other models (Gaussian fits, pairs of straight lines) did not improve the outcome of this analysis. The sample of cells for which synaptic responses were considered in this study therefore consists of 74 cells.

Cluster Analysis

We performed a cluster analysis in order to determine whether neurons' visual properties could lead to the segregation of different functional cell classes. The usefulness of a cluster analysis is to reveal categories using multiple variables, especially when such categories are not visible when using one variable only. Even in the absence of clear gaps in the distribution for one or several variables, presence of clusters indicates that cells that occupy a particular range in the distribution for one variable also occupy one restricted range for other variables. In order to give equal weight to each of them, the 3 variables used to characterize neurons' spiking response selectivity (RURA, HWHH, DnSI) have been used after normalization to their *z* scores. Cluster analysis is valid only if the variables in use show minimal correlation between each other. This was the case here (r^2 were 0.15, 0.001, and 0.039 between HWHH and RURA, between HWHH and DnSI, and between RURA and DnSI, respectively). The outcome of the cluster analysis, performed using Statistica® software, is represented as a hierarchical tree (Fig. 6), constructed using Ward's method of amalgamation. The vertical distance corresponds to the linkage distance calculated as Euclidean distance.

Statistics

Unless otherwise stated, analysis of variance tests were used to examine differences in orientation tuning between cell types or between clusters, and the Fisher's post hoc protected least significant difference test was thereafter applied to compare groups 2 by 2. Unless otherwise stated, data are reported as mean ± SD and the relationships between synaptic and spiking responses were examined using linear regression analysis.

Results

The present study is based on 111 cells that have been identified in terms of electrophysiological cell classes and that also presented significant spiking response in orientation tuning protocols. The 111 neurons were electrophysiologically classified as IB cells (n = 15), CH cells (n = 19), RS cells (n = 58), and FS cells (n = 19) (Nowak et al. 2003; see Methods and Fig. 1).

Examples Illustrate a Broad Range of Orientation Tuning and Direction Selectivity

An example of orientation tuning in an FS cell is presented in Figure 2. In this as well as in all the other cells, orientation selectivity was probed using bars drifting through the receptive field. The spiking responses are shown as PSTHs (Fig. 2*A*), and the synaptic responses are shown as membrane potential averages for the 16 different stimuli (Fig. 2*B*). The mean firing rate (spontaneous activity subtracted) and the mean membrane potential (resting membrane potential subtracted) were calculated for each orientation and are presented as data points in Figure 2*C*. The data were fitted using pairs of Von Mises equation (see Methods), and the resulting best fitting lines are shown as continuous lines in Figure 2*C*. These data show that the spiking response in this FS cell was sharply tuned for

orientation with a strong response at 315° and that it was also strongly direction selective. Responses at the membrane potential level were less sharply tuned and included a relatively large depolarization for orientations that did not induce spiking responses.

In sharp contrast to the cell in Figure 2, the FS cell whose responses are shown in Figure 3 appeared to be weakly selective for orientation. Spike discharges of similar amplitudes were obtained with all orientations and directions of the drifting bar (Fig. 3*A*). Membrane potential averages also revealed substantial depolarization in response to all stimuli (Fig. 3*B*). Fitting of the mean firing rate as a function of orientation (Fig. 3*C*) quantitatively supported the broadness of tuning in this cell: the RURA (see Methods) represented >60% of the maximal response and the HWHH of the tuned response component was 45°. The synaptic response (Fig. 3*C*) was even less orientation selective, with a larger RURA (71%) and a wider HWHH (47°).

Additional examples of orientation tuning curves are displayed as polar plots in Figure 4. They illustrate the range of orientation and direction selectivity found in the 4 electrophysiological cell classes. This shows that, within a given cell class, some cells may be strongly direction selective (Fig. 4*B*,*E*,*H*,*K*), whereas others are less or not at all (Fig. 4*A*,*D*,*G*,*J*). Some cells may be very sharply tuned for orientation (Fig. 4*A*,*D*,*G*,*J*), whereas others appear to be less so (Fig. 4*C*,*F*,*I*,*L*). However, the FS cell class appears unique in that it includes cells that are very weakly selective (Figs 3 and 4*L*), in a way not encountered in any other cell class.

Orientation and Direction Selectivity in Different Electrophysiological Cell Classes

Our analysis revealed that, at the population level, FS cells are less orientation and direction selective than the other cell classes. To examine differences and similarity in orientation and direction selectivity, we quantified the responses and examined 3 different variables. The first variable we examined was the RURA. The RURA represents the amount of response that lacks orientation and direction selectivity (y_0 in the equation fit), expressed relative to the response amplitude obtained for the preferred orientation ($y_0/(y_0 + A_1)$). The cumulative distribution in Figure 5*A* shows that, as expected, this unselective response amplitude is close to zero for most cells (indicating that most cells are highly selective). A small number of cells showed negative values, indicating firing rate reduction below spontaneous activity level for nonoptimal orientations. The most noticeable feature of the distribution is the presence of a proportion of FS cells that showed RURA values larger than that observed in the other cell classes.

The mean value for this measure of response unselectivity (Fig. 5*B* and Table 1) was significantly larger in FS cells in comparison with RS and CH cells ($P < 0.0001$ and $P = 0.0015$, respectively). On average, the amplitude of the nonselective response in FS cells represented 18.1 ± 25.7% of the response amplitude obtained with the preferred orientation and direction. IB cells showed an unselective response amplitude that did not differ significantly from that of FS cells ($P = 0.07$), although the FS distribution is clearly more skewed (Fig. 5*A*).

The second variable we examined was the HWHH of the orientation tuning curves. The HWHH provides a measure of the sharpness of orientation selectivity for the component of the response that is orientation selective (A_1 and A_2 parameters in the equation fit). At the population level, we found that FS cells showed HWHH larger than those of the other cell classes. Figure 5*C* shows that the HWHHs were distributed similarly between CH, IB, and RS cells, except for a small number of RS cells with a large HWHH. HWHH did not differ significantly between these 3 cell types. In contrast, the cumulative distribution for FS cells is shifted relative to that of the other cells, and the HWHH was found to be significantly

larger in FS cells in comparison with CH ($P = 0.0008$), IB ($P = 0.007$), or RS ($P = 0.0004$) cells. The mean value for FS cells was 31.9 ± 13.1 deg, a value that was 1.4–1.5 times larger than the HWHH found in the other cell types (Fig. 5*D* and Table 1). Thus, FS cells not only show larger unselective response amplitude but also their selective response component appears to be less sharp than in other cell types.

Finally, the DnSI (see Methods), the third variable we examined, was significantly larger in FS cells in comparison with RS ($P = 0.03$) and CH cells ($P = 0.01$) (Fig. 5*E*,*F* and Table 1), meaning that FS cells are less direction selective on average. IB cells showed intermediate values of DnSI that did not differ from that in the other classes.

Altogether, these data show that CH and RS cells appear to be slightly more direction selective than FS cells. More importantly, it appears that, as a group, FS cells appear to be consistently less orientation selective than other cell types.

Electrophysiological Cell Classes Versus Receptive Field Types

Previous studies have repeatedly reported differences in orientation selectivity between simple and complex cells (Albus 1975; Gizzi et al. 1990; Henry et al. 1974; Ikeda and Wright 1975; Leventhal and Hirsch 1978; Rose and Blakemore 1974; Schiller et al. 1976b; Skottun et al. 1987). It was therefore important to determine 1) whether RF types were distributed evenly between electrophysiological cell classes and 2) if this was not the case, whether differences between electrophysiological cell classes reflected differences between simple and complex cell proportions.

In our sample, 49 cells displayed complex receptive fields and 48 had simple receptive fields (14 cells were lost before completion of RF type identification; see Methods). RF type distribution for each of the electrophysiological cell classes is summarized in Table 2. Chi-square test revealed a significant difference between cell classes ($P = 0.01$). A posteriori contribution showed that IB cells were more often complex ($z = 2.6$), and RS more often simple ($z = 2.4$), than expected if electrophysiological cell classes and RF types were independent. Proportions of simple and complex CH cells were very close to the 50/50 found for the whole sample. Finally, although 65% of the FS cells were complex, this proportion was not significantly different from that observed for the whole population ($z = 1.3$).

On the other hand, we found no strong difference in orientation and direction selectivity between simple and complex cells (not illustrated). HWHH and DnSI were not significantly different between simple and complex cells ($P = 0.9$ for both parameters) and only RURA showed a trend ($P = 0.07$) with complex cells having a larger mean value—likely reflecting the fact that most FS cells with weak orientation selectivity were complex (see below). Given the lack of strong difference between simple and complex cells, we have not examined further the interaction between RF types and orientation selectivity.

Cluster Analysis Reveals a Subgroup of Weakly Selective FS Cells

We next examined the relationship between direction and orientation selectivity and cell classes in the reverse direction: rather than starting from the electrophysiological cell classes, we tried to determine whether orientation and direction selectivity would naturally generate different cell classes and how these cell classes would correspond to the ones defined electrophysiologically. More precisely, we wanted to bring an objective basis to our impression that some FS cells were less selective than the remaining neurons. For this purpose, we performed a cluster analysis using the 3 measures of response selectivity presented above.

The result of the cluster analysis is shown as a hierarchical tree in Figure 6*A*. There are 3 well-isolated clusters that are issued from branches that separate from each other at relatively large aggregation distances (~40 and 30). The second cluster is the smallest and contains 8.1% of the cells. Clusters 1 and 3 are similar in sizes and contain 42.3% and 49.5% of the cells, respectively.

The 3 clusters differed strongly in terms of orientation and direction selectivity (Table 3). Figure 6*B* shows distribution histograms for HWHH in the first column, RURA in the second column, and DnSI in the third column. The first row of histograms shows data for all the cells together, and distributions for the clusters 1, 2, and 3 are presented in the second, third, and fourth row. Cluster 3 contains the most selective cells, with all 3 distributions skewed toward selective, indicating that they are both orientation and direction selective. In contrast, cluster 2 contains the least selective cells, with all 3 distributions biased toward nonselective, indicating that this group is only weakly selective for orientation or direction. Cluster 1 is distinct in that it contains cells that have a low HWHH and unselective response measure, indicating that they are selective for stimulus orientation, but relatively high DnSI, indicating weak direction selectivity. Differences between clusters were significant (see Table 3; for HWHH: cluster 2 > cluster 1 [$P < 0.0001$] and cluster 3 [$P < 0.0001$]; for RURA: cluster 2 > cluster 1 [$P < 0.0001$] and cluster 3 [$P < 0.0001$]; for DnSI: cluster 3 < cluster 1 [$P < 0.0001$] and cluster 2 [$P < 0.0001$]).

We next examined the cluster content with respect to the 4 electrophysiological cell classes. As shown in Figure 7*A*, clusters 1 and 3 appeared to be composed of all the cell types we have identified in proportions roughly similar to those found for the whole population. On the other hand, cluster 2, in which cells are relatively unselective for both orientation and direction, contains a high percentage (78%) of FS cells, even though they are only 17% of the population overall (Fig. 7*A*). Conversely, although RS cells represented the dominant cell type in the whole population, they represented only 11% of the cells in cluster 2. Chi-square test confirmed significantly different cell type distributions in the different clusters ($P < 0.0001$). A posteriori contributions showed that proportions of cells in cluster 1 were not different from that expected if cell class and clusters were independent. However, CH cells were slightly more abundant ($z = 2.3$) and FS cells slightly less abundant ($z = -2.2$) in cluster 3, in comparison with expected values. Thus, only 5 out of 19 FS cells could be considered as direction selective (FS cells of cluster 3, with DnSI <50%). But by far the largest difference from expectation was the large proportion of FS cells in cluster 2 ($z = 5.0$).

The cell shown as an example in Figure 3 corresponded to one of the broadly tuned FS cells of cluster 2, as was the cell shown in Figure 4*L*. Additional examples of broadly tuned FS cells from cluster 2 are also presented as polar plots in Figure 8*C*,*D*. Examples of orientation selective, but not direction selective, FS cells belonging to cluster 1 are depicted in Figure 4*J* as well as Figure 8*A*,*B*. Finally, FS cells belonging to cluster 3 (orientation and direction selective neurons) appear in Figures 2, 4*K*, and 8*E*,*F*.

The scattergram shown in Figure 7*B* shows, as expected given the functional properties of cat area 17, that most cells exhibited significant orientation tuning, possessing low values of both HWHH and RURA. Fewer cells, belonging to all 3 clusters, exhibited relatively large (>35 deg) values of HWHH. What most clearly characterizes cluster 2 is the co-occurrence of both a large HWHH and a large RURA. Interestingly, the 2 non-FS cells in cluster 2 have values that are on the margin of this cluster (Fig. 7*B*).

Among our sample of 19 FS cells, 2 have been intracellularly labeled with biocytin. Both cells have been found in layer 4 and showed morphological features of inhibitory neurons.

Both possessed complex RFs. One was orientation but not direction selective and belonged to cluster 1, whereas the other was weakly selective and belonged to cluster 2.

Among the 7 cells of cluster 2 for which this information was available, RFs were found to be of the complex type in 6 (1 IB and 5 FS cells). Thus, most of the broadly tuned FS cells appear to possess complex receptive fields. Receptive field types are further illustrated in Supplementary Material, Figure 1 for 6 of the 7 FS cells of cluster 2. In 5 cells, RF type was determined from the response modulation to drifting sinewave gratings presented with the optimal orientation and spatial frequency. For 4 of these 5 cells, the relative modulation index (see Methods) was <1, indicating these cells were complex (Supplementary Material, Fig. 1*A*,*B*,*C*,*E*). For the last of these 5 cells, the modulation index was just above 1 (Supplementary Material, Fig. 1*D*), suggesting this cell was simple but not as strongly so as typical simple cells. The RF type was also determined for a sixth cell using the response to bright and dark moving bar. PSTHs show that the dark bar response completely overlapped the bright bar response, indicating this cell was complex (Supplementary Material, Fig. 1*F*). The RF type for the seventh broadly tuned FS cell of cluster 2 could not be determined.

Thus, our analysis has revealed the existence of a subgroup of cells that are characterized by weak orientation and direction selectivity. This subgroup consists almost entirely of FS neurons with complex RF, although other FS cells exhibit stronger orientation and direction selectivity.

Unselective Response Amplitude in the Membrane Potential

To examine the mechanisms responsible for the within- and between- electrophysiological cell type differences in orientation and direction selectivity, we first examined the properties of this selectivity in the membrane potential responses (n = 74 cells; see Methods). The examples shown in Figures 2, 3, 4, and 8 show that, in most cells, responses at the membrane potential level were less selective than those exhibited in the spiking responses: postsynaptic responses were very often >0 mV with all stimuli resulting in an unselective response amplitude >0% in most cells; sharpness of the tuned response component was often less than that for the spiking response, and direction selectivity was also less pronounced in the membrane potential response. This also was the case at the population level for the whole population as well as within each cell types (Table 4, to be compared with Table 1). With the exception of direction selectivity in IB cells, the 3 variables used to quantify orientation and direction selectivity were found to display higher values for postsynaptic membrane response in comparison with spiking responses ($P < 0.05$, paired t-test, not illustrated). This is in accordance with earlier studies showing less selectivity for membrane potential versus action potential responses (Carandini and Ferster 2000; Creutzfeldt et al. 1974; Hirsch et al. 2003; Jagadeesh et al. 1997; Monier et al. 2003; Nelson et al. 1994; Priebe and Ferster 2005; Schummers et al. 2002; Volgushev et al. 2000, 2002). We next examined whether differences observed for spiking responses between cell classes and differences observed between clusters could be correlated with differences in the membrane potential responses.

Plotting results for spike versus membrane potential responses for the 3 measures of orientation and direction selectivity reveal significant, but low correlations (Figs 9–11). For the first measure, the RURA (Fig. 9*A*), the unselectivity of the spike response increased in relation to that in the membrane potential response with a regression coefficient of 0.54 (R^2 = 0.285; $P < 0.0001$).

Although the RURA for postsynaptic responses did not differ significantly between cell classes (Fig. 9*B* and Table 4), it was significantly larger for cells in cluster 2 compared with cells in clusters 1 and 3 (Fig. 9*C* and Table 5). Thus, the weak selectivity of the action

potential responses in cluster 2 cells is echoed by a weak selectivity in their postsynaptic membrane potential responses.

Sharpness of Orientation Selectivity in the Postsynaptic Response

We carried out the same kind of analysis on the HWHH, which is presented in Figure 10. However, a complication arose due to the presence of cells for which the postsynaptic responses were not considered orientation selective (RURA >80%). These cells have been given, arbitrarily, an HWHH of 90 deg. For this reason, median values rather than means have been considered and statistical comparisons have been made using nonparametric tests.

We found a relatively weak linear relation ($R = 0.50$) between HWHH in membrane potential and action potential response (Fig. 10*A*), although it was highly significant ($P < 0.0001$, $R^2 = 0.255$). In the extreme, there are numerous cells whose sharply tuned spiking responses appear to arise from broadly tuned or even completely untuned membrane potential responses (Fig. 10*A*).

HWHH of tuning curves fitted to membrane potential responses was the largest in FS cells (median 45 deg; Fig. 10*B* and Table 4). Values for FS cells were significantly ($P = 0.008$, Mann-Whitney *U*-test) larger than those for RS cells (median 35.9 deg) but did not differ significantly from those in CH (median 36 deg) and IB cells (median 42.5 deg).

When clusters defined by orientation and direction selectivity are compared (Fig. 10*C* and Table 5), there does not appear to be a significant difference between cluster 2 and the other clusters, despite the fact that cluster 2 contains cells with large HWHH for membrane potential responses (median 46.6 deg). On the other hand, HWHH for cells in cluster 3 was significantly larger than that for cells in cluster 1 ($P = 0.04$, medians 42.1 and 35.1 deg, respectively), a difference that did not show up in the spiking responses (Fig. 6*B*).

These data show that differences in HWHH found between cell types for spiking responses is partially consistent with differences found in the synaptic responses.

Direction Selectivity in the Postsynaptic Response

Direction selectivity for spiking responses is significantly, but weakly ($R = 0.53$), correlated with direction selectivity for synaptic responses (Fig. 11*A; *$R^2 = 0.281$). Comparing the membrane potential DnSI between different cell classes (Fig. 11*B* and Table 4) revealed a significant difference between FS and RS cells ($P = 0.03$) but not between CH and FS cells ($P = 0.18$). Cells in cluster 3, which are characterized by a high degree of direction selectivity in their spike responses, also exhibit a higher direction selectivity (lower DnSI) in their synaptic responses than the other 2 clusters (Fig. 11*C* and Table 5; $P < 0.0001$ between clusters 1 and 3, $P = 0.047$ between clusters 2 and 3). Therefore, differences in direction selectivity between cell types and between clusters are visible in the synaptic responses (Tables 4 and 5), although these differences are less large than those exhibited by the spiking responses (Tables 1 and 3). This suggests that differences in membrane potential response only partially explain differences in spiking response.

Gamma-Range Fluctuations Do Not Contribute to Differences in Orientation and Direction Selectivity between Cell Classes

High frequency fluctuations are commonly observed in the membrane potential of cortical neurons during spontaneous activity and are often found to increase in the presence of visual stimulation. Here we examined whether occurrence and amplitude of gamma-range fluctuations contributed to the differences in orientation and direction selectivity observed between cell classes and between functionally defined clusters.

The results are detailed in Supplementary Material. In short, we found that occurrence and amplitude of gamma-range fluctuations differed strongly between electrophysiological cell types. However, these differences did not appear to parallel differences in orientation and direction selectivity. In particular, high-frequency membrane potential fluctuations do not provide an explanation as to why a subpopulation of FS cells exhibit weak orientation and direction selectivity.

Contribution of Spike Threshold

In addition to synaptic mechanisms, mechanisms intrinsic to the recorded cells might contribute to orientation selectivity. Spike threshold, in particular, has been shown to contribute to the sharpening of orientation and direction selectivity in the spiking responses relative to the postsynaptic responses (Azouz and Gray 2003; Carandini and Ferster 2000; Jagadeesh et al. 1997; Volgushev et al. 2000). Therefore, variability in spike threshold between cell types could explain some of the variability in orientation selectivity: through a simple “iceberg” effect, cells in which the resting membrane potential is close to spike threshold are expected to yield orientation and direction selectivity closer to the one exhibited at the membrane potential level. However, cells in which the spike threshold is far from the resting membrane potential are expected to fire only when the synaptic responses are large enough to reach that threshold, thus leading to a relative sharpening of orientation and direction selectivity. This would predict that FS cells have a lower spike threshold in comparison with other cell types.

Spike threshold was indeed found to differ between cell types (Fig. 12*A*), with FS cells characterized by the lowest spike threshold (8.6 ± 4.6 mV above resting membrane potential, $n = 17$). This was significantly lower than the value obtained in CH cells ($P = 0.008$) and in RS cells ($P = 0.04$). CH cells displayed the highest spike threshold (14.7 ± 5.0 mV, $n = 18$). This value was significantly ($P = 0.02$) larger than that obtained in RS cells (11.7 ± 5.0 mV, $n = 51$). IB cells showed a spike threshold similar to that in RS cells (11.3 ± 6.5 mV, $n = 15$), but, owing to larger variability (or smaller samples size), they were just above the margin of a significant difference with CH cells ($P = 0.06$). Differences we report here are comparable with those reported previously by Azouz and Gray (2000). When all cells are considered together, the mean spike threshold was 11.7 ± 5.4, a value very similar to that reported by Volgushev et al. (2002): 11.8 mV.

Differences in spike threshold were also obtained when comparing the orientation/direction selectivity-defined clusters (Fig. 11*B*). Cells in cluster 2 (which consists mostly of weakly selective FS cells) showed a spike threshold more depolarized than those in cluster 3 ($P = 0.04$; 7.5 ± 3.4 mV, $n = 7$, vs. 12.2 ± 5.9 mV, $n = 52$) and cluster 1, although the latter was not quite statistically significant ($P = 0.06$, 11.8 ± 4.9 mV, $n = 42$).

Spike threshold therefore appears to differ to some extent between cell types and between clusters. The general tendency was that of a lower spike threshold for cells that were less orientation selective (FS cells or cluster 2 cells).

We next examined whether differences in spike threshold could predict variability in orientation and direction selectivity. For this purpose, we first used a simple linear regression analysis (not illustrated). A significant relationship was found between spike threshold and RURA ($P = 0.04$). However, the strength of the relationship appeared to be rather weak, with a correlation, R, of only 0.18 ($R^2 = 0.034$). Spike threshold was also significantly correlated with HWHH ($P < 0.001$), with a mild $R = -0.39$ and $R^2 = 0.152$. This was an inverse relationship, such that cells with higher spike threshold tended to display lower HWHH. Finally, spike threshold and DnSI did not appear to be significantly correlated ($P = 0.997$).

We pursued our examination of the effects of spike threshold on orientation and direction selectivity using multiple regression analysis. First of all, we examined the RURA for spike response using both spike threshold and RURA for membrane potential response as independent variables. Including spike threshold improved the relationship compared with the one without spike threshold (illustrated in Fig. 9*C*). The *R* increased from 0.53 to 0.61, and the R^2 increased from 0.285 to 0.371.

Likewise, when HWHH for spike response was analyzed against spike threshold and HWHH for membrane potential responses together, the regression quality improved in comparison with the one using HWHH alone (Fig. 10*C*). *R* increased from 0.50 to 0.65 and R^2 from 0.255 to 0.418.

The same kind of analysis applied to direction selectivity did not have the same favorable outcome. Direction selectivity for spike response was not better predicted by a model including action potential threshold in addition to synaptic response direction selectivity (R^2 remained nearly unchanged, from 0.281 to 0.271).

Altogether, our results show that spike threshold differs between cell types and clusters and tends to be lower in cells with less orientation selectivity. Spike threshold does not seem to have an impact on direction selectivity, but variability in spike threshold does contribute to the variability in unselective response amplitude and in HWHH, although this contribution is less than that of synaptic responses.

Contribution of Cell Excitability

In association with spike threshold, another mechanism could contribute to the differences we have reported here, which is the difference in excitability between cell types. Indeed, one defining feature of FS cells is the steep slope of the relationship between current intensity and firing rate (e.g., McCormick et al. 1985; Nowak et al. 2003). This implies that, for an equivalent synaptic current, response strength should be higher in FS cells compared with other cell types.

As a measure of response strength, we considered not the mean firing rate but the mean number of spikes induced by each presentation of the best orientation (see Methods). As summarized in Figure 13*A*, FS, CH, and IB cells did not differ significantly. However, the mean number of spikes per stimulus was significantly lower in RS cells (15.2 ± 14.4 spikes per stimulus) in comparison with FS cells (24.7 ± 16.6 spikes per stimulus, $P = 0.03$), CH cells (31.9 ± 19.9 spikes per stimulus, $P = 0.0002$) and IB cells (27.5 ± 15.2, $P = 0.009$). There is some difficulty in interpreting this result because it is unclear whether all spikes in a burst count or whether the relevant “event” is the full burst in IB and CH cells. However, the difference found between RS and FS cells is not complicated by this consideration.

Rather than resulting from differences in intrinsic properties, it could be argued that the larger response strength exhibited by FS cells simply reflected larger synaptic responses, in comparison with RS cells. This was found not to be the case. If at all, there was a tendency ($P = 0.06$) for synaptic responses to be larger in RS cells (5.1 ± 2.2 mV) compared with FS cells (3.8 ± 1.8 mV) (not illustrated).

Although cell excitability differed between electrophysiological cell classes, this did not appear to contribute to differences in orientation and direction selectivity. First of all, when considering orientation/direction-based clusters instead of electrophysiological cell types (Fig. 13*B*), no significant difference could be found between weakly and strongly selective cells. Mean numbers of spikes per stimuli were 22.3 ± 18.5 spikes per stimulus in cluster 1, 23.5 ± 14.3 spikes per stimulus in cluster 2, and 21.1 ± 13.6 spikes per stimulus in cluster 3.

In addition, including response strength in multiple regression analysis did not improve the quality of the relationship between synaptic and spiking response tuning indices.

In summary, there appears to be a difference in excitability between cell types, with FS being 1.6 times more responsive than RS cells; yet this difference does not seem to explain differences in orientation selectivity because cells in cluster 2 (weakly selective cells) showed no difference with cells in the other clusters.

Discussion

Our study demonstrates an association between electrophysiological cell classes and orientation and direction selectivity. We have shown that, whereas RS, IB, and CH cells are similar, FS cells exhibit significantly less orientation and direction selectivity. This stems from the existence of a subgroup of FS cells that shows very weak orientation and direction selectivity, in accordance with earlier results obtained in rabbit area 17 on extracellularly recorded suspected interneurons (Swadlow and Weyand 1987) and in cat area 17 on intracellularly labeled interneurons (Hirsch et al. 2003). We further examined which mechanisms could lead to these differences. Occurrence and amplitude of gamma-range membrane fluctuations (detailed in Supplementary Material) and differences in intrinsic excitability did not appear to contribute to these differences. These differences could be accounted for, at least in part, by differences in both spike threshold and tuning of synaptic responses.

Receptive Field Properties of Electrophysiologically Defined Cell Classes

Examination of the RF type associated with each of the different electrophysiological cell classes shows that RS, CH, IB, and FS cells can be either simple or complex. However, significant interactions between cell class and RF type have been found in the case of IB and RS cells. As shown previously (Nowak et al. 2003; Contreras and Palmer 2003), IB cells most often possessed complex RFs, but some IB cells with simple RFs have also been encountered (Table 2). On the opposite, RS cells in the present and previous studies (Nowak et al. 2003) appeared to be more often simple than complex, although complex RS cells are far from being uncommon (Contreras and Palmer 2003; Nowak et al. 2003). Although it was initially reported that CH cells generally possess simple RFs (Gray and McCormick 1996, Nowak et al. 2003), the present study reveals approximately equal proportions of CH cells with simple and complex RFs, as also recently shown by Cardin et al. (2005). Finally, although 65% of the FS cells we recorded from were complex, this bias did not appear to be statistically significant. Thus, FS cells appear be either simple or complex in approximately equal proportions (as also shown by Azouz et al. 1997; Contreras and Palmer 2003). This is supported by studies combining morphological identification and RF characterization, which have shown that basket and clutch cells in cat area 17 can be either simple or complex (Ahmed et al. 1997; Azouz et al. 1997; Gabbott et al. 1988; Gilbert and Wiesel 1979; Hirsch et al. 2003; Kisvarday et al. 1987; Lin et al. 1979; Martin et al 1983, 1989; Martin 1988).

Beside RF type (and orientation and direction selectivity described in the present study), the only functional property that has been characterized and compared between different electrophysiological cell classes is their contrast-response function. Contreras and Palmer (2003) found clear differences between cell classes, with FS neurons displaying larger responses for all contrasts, in comparison with RS cells, without accompanying difference for synaptic responses. We also found that, in response to the same stimulus, response strength in FS cells was significantly larger than in RS cells (Fig. 13), without difference in the underlying mean synaptic response amplitude.

Orientation Selectivity in Inhibitory Neurons

The existence of cells in cat area 17 that lack clear orientation selectivity has been noticed in the past (Bullier and Henry 1979; Maldonado et al. 1997; Singer et al. 1975). In rabbit visual cortex, Swadlow and Weyand (1987) found nonoriented cells receiving monosynaptic inputs from the LGN, and these neurons resembled FS cells in their electrophysiological characteristics. Swadlow and Weyand (1987) and Swadlow (1988) further showed that these cells, also characterized by high spontaneous firing rates, additionally lacked direction selectivity. They also displayed high temporal frequency cutoffs and “motion-uniform” receptive fields (complex receptive fields). However, in cat area 17, the recording and morphological identification of interneurons have typically shown these cells to be orientation selective (Ahmed et al. 1997; Gabbott et al. 1988; Kisvarday et al. 1987; Martin et al. 1983, 1989). Indeed, we have found here that even the least selective FS cells show some degree of orientation bias. The reason why broadly tuned inhibitory neurons might have been missed in earlier studies could be the fact that orientation selectivity was essentially qualitatively assessed. Nevertheless, a previous quantitative study (Azouz et al. 1997), in which some of us were involved, failed to reveal any significant difference between FS and non-FS cells, although the sample of FS cells in Azouz et al. (1997) study was much smaller than in the present report. More recently, Hirsch et al. (2003), using intracellular labeling and recording, positively identified in layer 4 of cat area 17 simple inhibitory neurons that were orientation selective and complex inhibitory neurons that were not. The broadly tuned FS cells we report here are likely to correspond to the nonorientation selective, complex inhibitory neurons of layer 4 described by Hirsch et al. (2003).

Our data show that FS cells (especially those that constitute our functionally characterized cluster number 2) are less orientation and direction selective than the other cells. This was correlated with 2 factors: differences in spike threshold, which tends to be lower than in other cell classes or clusters, and differences in tuning for the synaptic responses, which tend to be broader than in the other cell classes or clusters. Sharpening of orientation and direction selectivity has been shown to depend on a nonlinear relationship between membrane potential and spike firing (Anderson, Lampl, Gillespie, and Ferster 2000; Priebe et al. 2004, 2005). Whether this relationship differs between the different electrophysiological cell types is a study of its own. However, if we conservatively assume identical transfer functions in all cell types, then tuning differences in the spike response would result, at a minimum, from the differences in synaptic response, as observed here.

What then needs to be explained is why the synaptic responses of a subgroup of FS cells are less tuned than that of other cells. Layer 4 neurons receive direct synaptic inputs from the LGN, and it may be suggested that the broadly tuned synaptic input to layer 4 FS cells is a result of these cells being “strongly dominated” by their thalamic inputs. This is consistent with the finding that cortical nonoriented FS cells display lower threshold for electrical activation from the LGN (Swadlow and Weyand 1987). Similar results were also obtained in the sensory cortex (Swadlow 1989). In addition, in vitro studies in somatosensory cortex have shown the excitatory drive produced by activating single thalamic axons to be 2–5 times larger in FS cells than in RS cells (Gabernet et al. 2005; Gibson et al. 1999; Porter et al. 2001). In addition to differences in amplitude, thalamic inputs on FS cells show faster kinetics than thalamic inputs on RS cells, enabling rapid activation of feedforward inhibition (Cruikshank et al. 2007). Paired extracellular recording in vivo and cross-correlation analysis also demonstrated a dominant contribution of thalamic inputs to the firing of FS neurons in the somatosensory cortex (Bruno and Simons 2002; Swadlow and Gusev 2002) and showed that the lack of direction selectivity in FS cells resulted from a nonspecific convergent input from thalamocortical neurons with different receptive field properties (Swadlow and Gusev 2002). In the visual system, LGN neurons are weakly orientation and direction selective. A dominant thalamic input could explain why FS cells show less

orientation and direction selectivity than excitatory neurons in layer 4. The orientation bias that these cells nevertheless express may be the consequence of a spatial bias in their thalamic inputs or of recurrent inputs they receive from orientation selective, excitatory cortical neurons. Alternatively, it could reflect the orientation bias exhibited by retinal ganglion cells and LGN neurons (Levick and Thibos 1980; Shou and Leventhal 1989; Soodak et al. 1987).

Weakly Selective FS Cells and the Generation of Direction Selectivity

Multiple studies have shown that direction selectivity is impaired when $GABA_A$-mediated inhibition is suppressed (Murthy and Humphrey 1999; Nelson 1991; Sato et al. 1995; Sillito 1975; Tsumoto et al. 1979). Direction selectivity might thus depend on direction selective inhibitory neurons (e.g., Maex and Orban 1996). On the other hand, we found that FS cells tended to be less direction selective than cells in the other classes; only 5 out of 19 FS cells could be considered as direction selective (FS cells of cluster 3, with DnSI <50%). One question that needs to be examined is whether direction selectivity can be obtained using inhibitory neurons that are not (or rarely) direction selective themselves (obviously we cannot exclude the involvement of non-FS inhibitory neurons that would be direction selective).

One class of model of direction selectivity corresponds to “recurrent” models, in which the role of recurrent intracortical excitation is emphasized (Douglas and Martin 1991; Suarez et al. 1995). The key feature of these “recurrent models” is that RFs of inhibitory neurons are slightly offset in space relative to the thalamic inputs received by excitatory neurons, in a configuration that has received some experimental support (Crook et al. 1996; Eysel et al. 1988), and direction selectivity is further amplified by recurrent intracortical excitation. In these models, inhibitory neurons need not be direction selective, even though they are instrumental in the appearance of this property.

Other proposed models correspond to linear direction selectivity models (Adelson and Bergen 1985; Watson and Ahumada 1985) that postulate that, in simple cells, direction selectivity derives from the combination of nondirectional RFs that have different response dynamics. Experimental studies have provided support for this class of models (Albrecht and Geisler 1991; De Valois et al. 2000; DeAngelis et al. 1993; Humphrey et al. 1998; Livingstone and Conway 2003; McLean and Palmer 1989; McLean et al. 1994; Peterson et al. 2004; Reid et al. 1991; Saul et al. 2005). The key feature of the linear direction selectivity models is that direction selectivity derives from the combination of nondirectional RFs that have different response latencies (De Valois et al. 2000; Livingstone and Conway 2003; Peterson et al. 2004; Saul et al. 2005). It is therefore conceivable that inhibition is involved in the generation of these first-order RFs, in such a way that inhibitory neurons need not be direction selective themselves.

Weakly Selective FS Cells and the Generation of Orientation Selectivity

Understanding how orientation selectivity is generated in visual cortex has been the subject of a great deal of research. According to the classical “feedforward” model of Hubel and Wiesel (1962), orientation selectivity in simple cells results from the elongation of their subregions, itself the consequence of the projection of thalamic neurons with spatially aligned receptive fields. However, contrast invariance of orientation selectivity (Skottun et al. 1987) cannot be accounted for by a purely excitatory feedforward model. On this regard, a “modified” feedforward model that includes antiphase inhibition has been shown to account for contrast-invariant orientation selectivity (Troyer et al. 1998; see also Hansel and van Vreeswijk 2002; Ursino and La Cara 2004). Contrast-invariant orientation selectivity has also been obtained in a model including nonselective inhibitory neurons (Lauritzen and

Miller 2003). Alternative to these models are various “recurrent” models of orientation selectivity (Ben-Yishai et al. 1995; Carandini and Ringach 1997; Douglas et al. 1995; McLaughlin et al. 2000; Somers et al. 1995; Teich and Qian 2006; Ursino and La Cara 2004; Vidyasagar et al. 1996). In these models, an initially weakly tuned thalamic input is sharpened through 2 processes: broadband inhibition and recurrent, “amplifying” excitation.

Both recurrent and feedforward models (with inhibition) require broadly tuned inhibition. In the feedforward model with inhibition (Troyer et al. 1998), the tuning of inhibitory neurons follows that of their thalamic inputs and therefore shows an untuned component whose amplitude grows with stimulus contrast. In recurrent models, broadly tuned inhibition is achieved through 2 different means: in the first, inhibition exhibits larger tuning width, compared with excitation, because inhibition comes from orientation selective inhibitory neurons with a large range of preferred orientations (Ben-Yishai et al. 1995; Douglas et al. 1995; Somers et al. 1995). Alternatively (McLaughlin et al. 2000), broadly tuned inhibition might emerge, within a network with realistic connectivity patterns, by virtue of different synaptic strengths for the different connections.

The results we obtained suggest yet another mechanism. Broadly tuned FS cells we recorded from here have the properties required for injecting broadly tuned inhibition, without resorting to particular intracortical connectivity scheme. Instead, their weak orientation selectivity may result, in addition to their low spike threshold, from particularly strong thalamic inputs, as demonstrated in the somatosensory cortex. This possibility is amenable to experimental scrutiny.

Supplementary Material

Refer to Web version on PubMed Central for supplementary material.

Acknowledgments

Funding

National Institutes of Health (DAM); Centre National de la Recherche Scientifique (LGN); Human Frontier Science Program and Ministerio de Ciencia y Tecnologia de España (MVSV).

References

Adelson EH, Bergen JR. Spatiotemporal energy models for the perception of motion. J Opt Soc Am A. 1985; 2:284–299. [PubMed: 3973762]

Ahmed B, Anderson JC, Martin KAC, Nelson JC. Map of the synapses onto layer 4 basket cells of the primary visual cortex of the cat. J Comp Neurol. 1997; 380:230–242. [PubMed: 9100134]

Albrecht DG, Geisler WS. Motion selectivity and the contrast-response function of simple cells in the visual cortex. Vis Neurosci. 1991; 7:531–546. [PubMed: 1772804]

Albus K. A quantitative study of the projection area of the central and the paracentral visual field in area 17 of the cat. II. The spatial organization of the orientation domain. Exp Brain Res. 1975; 24:181–202. [PubMed: 1218550]

Anderson JS, Lampl I, Gillespie DC, Ferster D. The contribution of noise to contrast invariance of orientation tuning in cat visual cortex. Science. 2000; 290:1968–1972. [PubMed: 11110664]

Angulo MC, Staiger JF, Rossier J, Audinat E. Developmental synaptic changes increase the range of integrative capabilities of an identified excitatory neocortical connection. J Neurosci. 1999; 19:1566–1576. [PubMed: 10024344]

Azouz R, Gray CM. Dynamic spike threshold reveals a mechanism for synaptic coincidence detection in cortical neurons in vivo. Proc Natl Acad Sci USA. 2000; 97:8110–8115. [PubMed: 10859358]

Azouz R, Gray CM. Adaptive coincidence detection and dynamic gain control in visual cortical neurons in vivo. Neuron. 2003; 37:513–523. [PubMed: 12575957]

Azouz R, Gray CM, Nowak LG, McCormick DA. Physiological properties of identified interneurons in cat striate cortex. Cereb Cortex. 1997; 7:534–545. [PubMed: 9276178]

Ben-Yishai R, Bar-Or RL, Sompolinsky H. Theory of orientation tuning in visual cortex. Proc Natl Acad Sci USA. 1995; 92:3844–3848. [PubMed: 7731993]

Bruno RM, Simons DJ. Feedforward mechanisms of excitatory and inhibitory cortical receptive fields. J Neurosci. 2002; 22:10966–10975. [PubMed: 12486192]

Bullier J, Henry GH. Ordinal position of neurons in cat striate cortex. J Neurophysiol. 1979; 42:1251–1263. [PubMed: 226663]

Calvin WH, Sypert GW. Fast and slow pyramidal tract neurons: an intracellular analysis of their contrasting repetitive firing properties in the cat. J Neurophysiol. 1976; 39:420–434. [PubMed: 1255231]

Carandini M, Ferster D. Membrane potential and firing rate in cat primary visual cortex. J Neurosci. 2000; 20:470–484. [PubMed: 10627623]

Carandini M, Ringach DL. Predictions of a recurrent model of orientation selectivity. Vision Res. 1997; 37:3061–3071. [PubMed: 9425519]

Cardin JA, Palmer LA, Contreras D. Stimulus-dependent gamma (30–50 Hz) oscillations in simple and complex fast rhythmic bursting cells in primary visual cortex. J Neurosci. 2005; 25:5339–5350. [PubMed: 15930382]

Cauli B, Audinat E, Lambolez B, Angulo MC, Ropert N, Tsuzuki K, Hestrin S, Rossier J. Molecular and physiological diversity of cortical nonpyramidal cells. J Neurosci. 1997; 15:3894–3906. [PubMed: 9133407]

Chagnac-Amitai Y, Luhmann HJ, Prince DA. Burst generating and regular spiking layer 5 pyramidal neurons of rat neocortex have different morphological features. J Comp Neurol. 1990; 296:598–613. [PubMed: 2358553]

Connors BW, Gutnick MJ, Prince DA. Electrophysiological properties of neocortical neurons in vitro. J Neurophysiol. 1982; 48:1302–1320. [PubMed: 6296328]

Contreras D, Palmer L. Response to contrast of electrophysiologically defined cell classes in primary visual cortex. J Neurosci. 2003; 23:6936–6945. [PubMed: 12890788]

Creutzfeldt OD, Kuhnt U, Benvento LA. An intracellular analysis of visual cortical neurones to moving stimuli: responses in a cooperative neuronal network. Exp Brain Res. 1974; 21:251–274. [PubMed: 4374364]

Crook JM, Kisvarday ZF, Eysel UT. GABA-induced inactivation of functionally characterized sites in cat visual cortex (area 18): effects on direction selectivity. J Neurophysiol. 1996; 75:2071–2088. [PubMed: 8734604]

Cruikshank SJ, Lewis TJ, Connors BW. Synaptic basis for intense thalamocortical activation of feedforward inhibitory cells in neocortex. Nat Neurosci. 2007; 10:462–468. [PubMed: 17334362]

De Valois RL, Albrecht DG, Thorell LG. The orientation and direction selectivity of cells in macaque visual cortex. Vision Res. 1982; 22:531–544. [PubMed: 7112953]

De Valois RL, Cottaris NP, Mahon LE, Elfar SD, Wilson JA. Spatial and temporal receptive fields of geniculate and cortical cells and direction selectivity. Vision Res. 2000; 40:3685–3702. [PubMed: 11090662]

DeAngelis GC, Ohzawa I, Freeman RD. Spatiotemporal organization of simple-cell receptive fields in the cat's striate cortex. II. Linearity of temporal and spatial summation. J Neurophysiol. 1993; 69:1118–1135. [PubMed: 8492152]

Deuchars J, Thomson AM. Innervation of burst firing spiny interneurons by pyramidal cells in deep layers of rat somatomotor cortex: paired intracellular recordings with biocytine filing. Neurosci. 1995; 69:739–755.

Douglas RJ, Koch C, Mahowald M, Martin KA, Suarez HH. Recurrent excitation in neocortical circuits. Science. 1995; 269:981–985. [PubMed: 7638624]

Douglas RJ, Martin KAC. A functional microcircuit for cat visual cortex. J Physiol. 1991; 440:735–769. [PubMed: 1666655]

Eysel UT, Muche T, Worgotter F. Lateral interactions at direction-selective striate neurones in the cat demonstrated by local cortical inactivation. J Physiol. 1988; 399:657–675. [PubMed: 3404472]

Ferster D, Miller KD. Neural mechanisms of orientation selectivity in the visual cortex. Annu Rev Neurosci. 2000; 23:441–471. [PubMed: 10845071]

Foehring RC, Lorenzon NM, Herron P, Wilson CJ. Correlation of physiologically and morphologically identified neuronal types in human association cortex in vitro. J Neurophysiol. 1991; 66:1825–1837. [PubMed: 1812219]

Gabbott PLA, Martin KAC, Whitteridge D. Evidence for the connections between a clutch cell and a corticotectal neuron in area 17 of the cat visual cortex. Proc R Soc Lond B Biol Sci. 1988; 233:385–391. [PubMed: 2899895]

Gabernet L, Jadhav SP, Feldman DE, Carandini M, Scanziani M. Somatosensory integration controlled by dynamic thalamocortical feed-forward inhibition. Neuron. 2005; 48:315–327. [PubMed: 16242411]

Gibson JR, Beierlein M, Connors BW. Two networks of electrically coupled inhibitory neurons in neocortex. Nature. 1999; 402:75–79. [PubMed: 10573419]

Gilbert CD, Wiesel TN. Morphology and intracortical projections of functionally characterized neurones in the cat visual cortex. Nature. 1979; 280:120–125. [PubMed: 552600]

Gizzi MS, Katz E, Schumer RA, Movshon JA. Selectivity for orientation and direction of motion of single neurons in cat striate and extrastriate visual cortex. J Neurophysiol. 1990; 63:1529–1543. [PubMed: 2358891]

Gray CM, McCormick DA. Chattering cells: superficial pyramidal neurons contributing to the generation of synchronous oscillations in the visual cortex. Science. 1996; 274:109–113. [PubMed: 8810245]

Gupta A, Wang Y, Markram H. Organizing principles for a diversity of GABAergic interneurons and synapses in the neocortex. Science. 2000; 287:273–278. [PubMed: 10634775]

Hansel D, van Vreeswijk C. How noise contributes to contrast invariance of orientation tuning in cat visual cortex. J Neurosci. 2002; 22:5118–5128. [PubMed: 12077207]

Heggelund P. Quantitative study of the discharge fields of single cells in cat striate cortex. J Physiol. 1986; 373:277–292. [PubMed: 3746674]

Henry GH, Dreher B, Bishop PO. Orientation specificity of cells in cat striate cortex. J Neurophysiol. 1974; 37:1394–1409. [PubMed: 4436709]

Hirsch JA. Synaptic integration in layer IV of the ferret striate cortex. J Physiol. 1995; 483:183–199. [PubMed: 7776231]

Hirsch JA, Martinez LM, Pillai C, Alonso JM, Wang Q, Sommer FT. Functionally distinct inhibitory neurons at the first stage of visual cortical processing. Nat Neurosci. 2003; 6:1300–1308. [PubMed: 14625553]

Hubel DH, Wiesel TN. Receptive fields, binocular interaction and functional architecture in the cat's visual cortex. J Physiol. 1962; 160:106–154. [PubMed: 14449617]

Humphrey AL, Saul AB, Feidler JC. Strobe rearing prevents the convergence of inputs with different response timings onto area 17 simple cells. J Neurophysiol. 1998; 80:3005–3020. [PubMed: 9862902]

Ikeda H, Wright MJ. Retinotopic distribution, visual latency and orientation tuning of 'sustained' and 'transient' cortical neurones in area 17 of the cat's visual cortex. Exp Brain Res. 1975; 22:385–398.

Jagadeesh B, Wheat HS, Kontsevich LL, Tyler CW, Ferster D. Direction selectivity of synaptic potentials in simple cells of the cat visual cortex. J Neurophysiol. 1997; 78:2772–2789. [PubMed: 9356425]

Kawaguchi Y. Physiological subgroups of nonpyramidal cells with specific morphological characteristics in layer II/III of rat frontal cortex. J Neurosci. 1995; 15:2638–2655. [PubMed: 7722619]

Kisvarday ZF, Martin KAC, Friedlander MJ, Somogyi P. Evidence for interlaminar inhibitory circuits in the striate cortex of the cat. J Comp Neurol. 1987; 260:1–19. [PubMed: 3597830]

Krimer LS, Zaitsev AV, Czanner G, Kroner S, Gonzalez-Burgos G, Povysheva NV, Iyengar S, Barrionuevo G, Lewis DA. Cluster analysis-based physiological classification and morphological

properties of inhibitory neurons in layers 2–3 of monkey dorsolateral prefrontal cortex. J Neurophysiol. 2005; 94:3009–3022. [PubMed: 15987765]

Larkman A, Mason A. Correlations between morphology and electrophysiology of pyramidal neurons in slices of rat visual cortex. I. Establishment of cell classes. J Neurosci. 1990; 10:1407–1414. [PubMed: 2332787]

Lauritzen TZ, Miller KD. Different roles for simple-cell and complex-cell inhibition in V1. J Neurosci. 2003; 23:10201–10213. [PubMed: 14614078]

Leventhal AG, Hirsch HVB. Receptive-field properties of neurons in different laminae of visual cortex of the cat. J Neurophysiol. 1978; 41:948–962. [PubMed: 681994]

Levick WR, Thibos LN. Orientation bias of cat retinal ganglion cells. Nature. 1980; 286:389–390. [PubMed: 7402319]

Lin CS, Friedlander MJ, Sherman SM. Morphology of physiologically identified neurons in the visual cortex of the cat. Brain Res. 1979; 172:344–348. [PubMed: 466478]

Livingstone MS, Conway BR. Substructure of direction-selective receptive fields in macaque V1. J Neurophysiol. 2003; 89:2743–2759. [PubMed: 12740412]

Maex R, Orban GA. Model circuit of spiking neurons generating directional selectivity in simple cells. J Neurophysiol. 1996; 75:1515–1545. [PubMed: 8727395]

Maldonado PE, Godecke I, Gray CM, Bonhoeffer T. Orientation selectivity in pinwheel centers in cat striate cortex. Science. 1997; 276:1551–1555. [PubMed: 9171056]

Martin KAC. The Wellcome Prize lecture. From single cells to simple circuits in the cerebral cortex. Q J Exp Physiol. 1988; 73:637–702. [PubMed: 3068702]

Martin KAC, Friedlander MJ, Alones V. Physiological, morphological, and cytochemical characteristics of a layer 1 neuron in cat striate cortex. J Comp Neurol. 1989; 282:404–414. [PubMed: 2715389]

Martin KAC, Somogyi P, Whitteridge D. Physiological and morphological properties of identified basket cells in the cat's visual cortex. Exp Brain Res. 1983; 50:193–200. [PubMed: 6641854]

Martinez LM, Wang Q, Reid RC, Pillai C, Alonso JM, Sommer FT, Hirsch JA. Receptive field structure varies with layer in the primary visual cortex. Nat Neurosci. 2005; 8:372–379. [PubMed: 15711543]

Mata ML, Ringach DL. Spatial overlap of ON and OFF subregions and its relation to response modulation ratio in macaque primary visual cortex. J Neurophysiol. 2005; 93:919–928. [PubMed: 15371494]

McCormick DA, Connors BW, Lighthall JW, Prince DA. Comparative electrophysiology of pyramidal and sparsely spiny stellate neurons of the neocortex. J Neurophysiol. 1985; 54:782–806. [PubMed: 2999347]

McLaughlin D, Shapley R, Shelley M, Wielaard DJ. A neuronal network model of macaque primary visual cortex (V1): orientation selectivity and dynamics in the input layer 4Calpha. Proc Natl Acad Sci USA. 2000; 97:8087–8092. [PubMed: 10869422]

McLean J, Palmer LA. Contribution of linear spatiotemporal receptive field structure to velocity selectivity of simple cells in area 17 of cat. Vision Res. 1989; 29:675–679. [PubMed: 2626824]

McLean J, Raab S, Palmer LA. Contribution of linear mechanisms to the specification of local motion by simple cells in areas 17 and 18 of the cat. Vis Neurosci. 1994; 11:271–294. [PubMed: 8003454]

Miller KD, Troyer TW. Neural noise can explain expansive, power-law nonlinearities in neural response functions. J Neurophysiol. 2002; 87:653–659. [PubMed: 11826034]

Monier C, Chavane F, Baudot P, Graham LJ, Frégnac Y. Orientation and direction selectivity of synaptic inputs in visual cortical neurons: a diversity of combinations produces spike tuning. Neuron. 2003; 37:663–680. [PubMed: 12597863]

Mountcastle VB, Talbot WH, Sakata H, Hyvärinen J. Cortical neuronal mechanisms in flutter-vibration studied in unanesthetized monkeys. Neuronal periodicity and frequency discrimination. J Neurophysiol. 1969; 32:452–484. [PubMed: 4977839]

Murthy A, Humphrey AL. Inhibitory contributions to spatiotemporal receptive-field structure and direction selectivity in simple cells of cat area 17. J Neurophysiol. 1999; 81:1212–1224. [PubMed: 10085348]

Nelson SB. Temporal interactions in the cat visual system. III. Pharmacological studies of cortical suppression suggest a presynaptic mechanism. J Neurosci. 1991; 11:369–380. [PubMed: 1992007]

Nelson SB, Toth L, Sheth B, Sur M. Orientation selectivity of cortical neurons during intracellular blockade of inhibition. Science. 1994; 265:774–777. [PubMed: 8047882]

Nowak LG, Azouz R, Sanchez-Vives MV, Gray CM, McCormick DA. Electrophysiological classes of cat primary visual cortical neurons in vivo as revealed by quantitative analysis. J Neurophysiol. 2003; 89:1541–1566. [PubMed: 12626627]

Nowak, LG.; Sanchez-Vives, MV.; McCormick, DA. Program No. 137.4 in Abstract Viewer/Itinerary Planner. Society for Neuroscience; Washington (DC): 2005a. Fast spiking neuron, an electrophysiologically identified subtype of inhibitory neuron, display broader orientation selectivity than other cell types in cat area 17.

Nowak LG, Sanchez-Vives MV, McCormick DA. Role of synaptic and intrinsic membrane properties in short term receptive field dynamics in cat area 17. J Neurosci. 2005b; 25:1866–1880. [PubMed: 15716423]

Palmer LA, Davis TL. Receptive-field structure in cat striate cortex. J Neurophysiol. 1981; 46:260–276. [PubMed: 6267213]

Peterson MR, Li B, Freeman RD. The derivation of direction selectivity in the striate cortex. J Neurosci. 2004; 24:3583–3591. [PubMed: 15071106]

Porter JT, Johnson CK, Agmon A. Diverse types of interneurons generate thalamus-evoked feedforward inhibition in the mouse barrel cortex. J Neurosci. 2001; 21:2699–6710. [PubMed: 11306623]

Priebe NJ, Ferster D. Direction selectivity of excitation and inhibition in simple cells of the cat primary visual cortex. Neuron. 2005; 45:133–145. [PubMed: 15629708]

Priebe NJ, Mechler F, Carandini M, Ferster D. The contribution of spike threshold to the dichotomy of cortical simple and complex cells. Nat Neurosci. 2004; 7:1113–1122. [PubMed: 15338009]

Reid RC, Soodak RE, Shapley RM. Directional selectivity and spatiotemporal structure of receptive fields of simple cells in cat striate cortex. J Neurophysiol. 1991; 66:505–529. [PubMed: 1774584]

Ringach DL, Hawken MJ, Shapley R. Dynamics of orientation tuning in macaque V1: the role of global and tuned suppression. J Neurophysiol. 2003; 90:342–352. [PubMed: 12611936]

Rose D, Blakemore C. An analysis of orientation selectivity in the cat's visual system. Exp Brain Res. 1974; 20:1–17. [PubMed: 4844166]

Sanchez-Vives MV, Nowak LG, McCormick DA. Membrane mechanisms underlying contrast adaptation in cat area 17 in vivo. J Neurosci. 2000; 20:4267–4285. [PubMed: 10818163]

Sato H, Katsuyama N, Tamura H, Hata Y, Tsumoto T. Mechanisms underlying direction selectivity of neurons in the primary visual cortex of the macaque. J Neurophysiol. 1995; 74:1382–1394. [PubMed: 8989379]

Saul AB, Carras PL, Humphrey AL. Temporal properties of inputs to direction-selective neurons in monkey V1. J Neurophysiol. 2005; 94:282–294. [PubMed: 15744011]

Schiller PH, Finlay BL, Volman SF. Quantitative studies of single-cell properties in monkey striate cortex. I. Spatiotemporal organization of receptive fields. J Neurophysiol. 1976a; 39:1288–1319. [PubMed: 825621]

Schiller PH, Finlay BL, Volman SF. Quantitative studies of single-cell properties in monkey striate cortex. II. Orientation specificity and ocular dominance. J Neurophysiol. 1976b; 39:1320–1333. [PubMed: 825622]

Schummers J, Marino J, Sur M. Synaptic integration by V1 neurons depends on location within the orientation map. Neuron. 2002; 36:969–978. [PubMed: 12467599]

Shapley R, Hawken M, Ringach DL. Dynamics of orientation selectivity in the primary visual cortex and the importance of cortical inhibition. Neuron. 2003; 38:689–699. [PubMed: 12797955]

Shou TD, Leventhal AG. Organized arrangement of orientation-sensitive relay cells in the cat's dorsal lateral geniculate nucleus. J Neurosci. 1989; 9:4287–4302. [PubMed: 2593002]

Sillito AM. The contribution of inhibitory mechanisms to the receptive field properties of neurones in the striate cortex of the cat. J Physiol. 1975; 250:305–329. [PubMed: 1177144]

Singer W, Tretter F, Cynader M. Organization of cat striate cortex: a correlation of receptive-field properties with afferent and efferent connections. J Neurophysiol. 1975; 38:1080–1098. [PubMed: 1177006]

Skottun BC, Bradley A, Sclar G, Ohzawa I, Freeman RD. The effects of contrast on visual orientation and spatial frequency discrimination: a comparison of single cells and behavior. J Neurophysiol. 1987; 57:773–786. [PubMed: 3559701]

Skottun BC, De Valois RL, Grosof DH, Movshon JA, Albrecht D, Bonds AB. Classifying simple and complex cells on the basis of response modulation. Vision Res. 1991; 31:1079–1086. [PubMed: 1909826]

Somers DC, Nelson SB, Sur M. An emergent model of orientation selectivity in cat visual cortical simple cells. J Neurosci. 1995; 15:5448–5465. [PubMed: 7643194]

Sompolinsky H, Shapley R. New perspectives on the mechanisms for orientation selectivity. Curr Opin Neurobiol. 1997; 7:514–522. [PubMed: 9287203]

Soodak RE, Shapley RM, Kaplan E. Linear mechanism of orientation tuning in the retina and lateral geniculate nucleus of the cat. J Neurophysiol. 1987; 58:267–275. [PubMed: 3655866]

Suarez H, Koch C, Douglas RJ. Modeling direction selectivity of simple cells in striate cortex within the framework of the canonical microcircuit. J Neurosci. 1995; 15:6700–6719. [PubMed: 7472430]

Swadlow HA. Efferent neurons and suspected interneurons in binocular visual cortex of the awake rabbit: receptive fields and binocular properties. J Neurophysiol. 1988; 59:1162–1187. [PubMed: 3373273]

Swadlow HA. Efferent neurons and suspected interneurons in S-1 vibrissa cortex of the awake rabbit: receptive fields and axonal properties. J Neurophysiol. 1989; 62:288–308. [PubMed: 2754479]

Swadlow HA, Gusev AG. Receptive-field construction in cortical inhibitory interneurons. Nat Neurosci. 2002; 5:403–404. [PubMed: 11967546]

Swadlow HA, Weyand TG. Corticogeniculate neurons, corticotectal neurons, and suspected interneurons in visual cortex of awake rabbit: receptive field properties, axonal properties, and effects of EEG arousal. J Neurophysiol. 1987; 57:977–1001. [PubMed: 3585466]

Swindale NV. Orientation tuning curves: empirical description and estimation of parameters. Biol Cybern. 1998; 78:45–56. [PubMed: 9518026]

Teich AF, Qian N. Comparison among some models of orientation selectivity. J Neurophysiol. 2006; 96:404–419. [PubMed: 16625000]

Troyer TW, Krukowski AE, Priebe NJ, Miller KD. Contrast-invariant orientation tuning in cat visual cortex: thalamocortical input tuning and correlation-based intracortical connectivity. J Neurosci. 1998; 18:5908–5927. [PubMed: 9671678]

Tsumoto T, Eckart W, Creutzfeldt OD. Modification of orientation sensitivity of cat visual cortex neurons by removal of GABA-mediated inhibition. Exp Brain Res. 1979; 34:351–363. [PubMed: 421752]

Ursino M, La Cara GE. Comparison of different models of orientation selectivity based on distinct intracortical inhibition rules. Vision Res. 2004; 44:1641–1658. [PubMed: 15136001]

Vidyasagar TR, Pei X, Volgushev M. Multiple mechanisms underlying the orientation selectivity of visual cortical neurones. Trends Neurosci. 1996; 19:272–277. [PubMed: 8799969]

Volgushev M, Pernberg J, Eysel UT. Comparison of the selectivity of postsynaptic potentials and spike responses in cat visual cortex. Eur J Neurosci. 2000; 12:257–263. [PubMed: 10651880]

Volgushev M, Pernberg J, Eysel UT. A novel mechanism of response selectivity of neurons in cat visual cortex. J Physiol. 2002; 540:307–320. [PubMed: 11927689]

Watson AB, Ahumada AJ Jr. Model of human visual-motion sensing. J Opt Soc Am A. 1985; 2:322–341. [PubMed: 3973764]

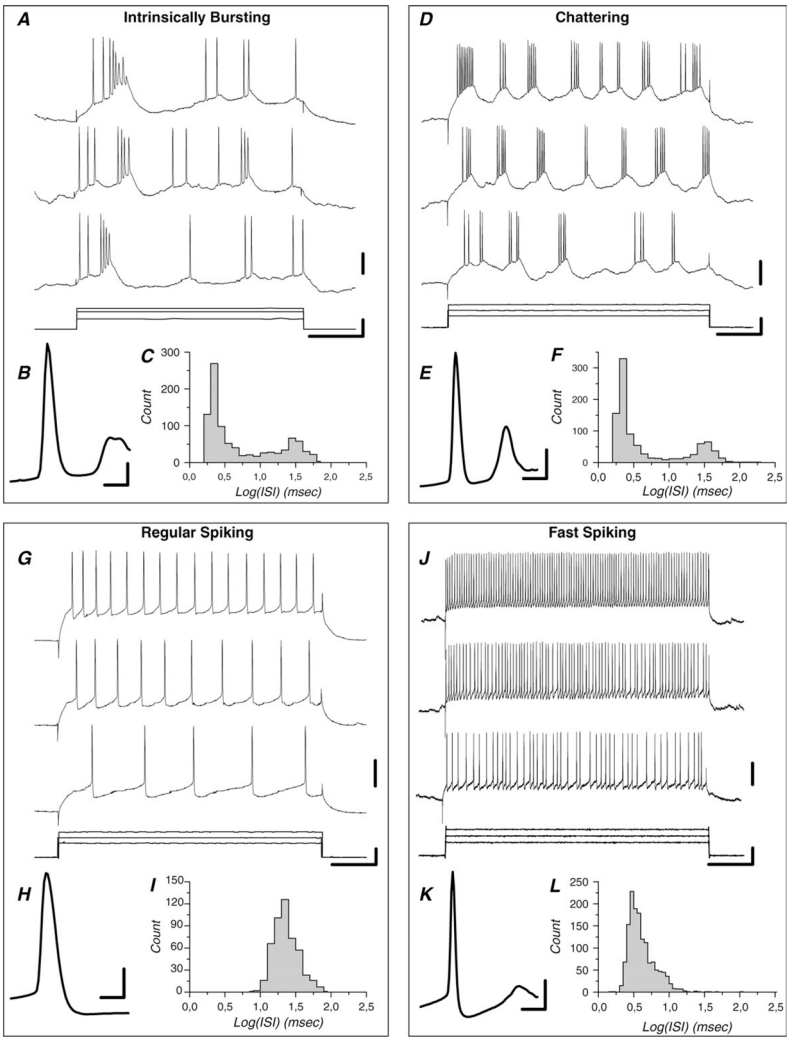

Figure 1.

Representative examples of the 4 different cell classes that can be identified in cat area 17 by their electrophysiological features. (*A–C*) IB cell. (*D–F*) CH cell. (*G–I*) RS cell. (*J–K*) FS cell. Log(ISIs) are unimodal in nonburst-generating neurons (*I*, *L*) and bimodal in burst-generating neurons (*C*, *F*). Action potentials are thinner in the CH cell (*E*) and in the FS cell (*K*) in comparison with the IB cell (*B*) and the RS cell (*H*). Bursts discharge tends to inactivate in the IB cell (*A*) but persists for the whole current pulse duration in the CH cell (*D*). The RS cell shows firing rate adaptation (*G*) but the FS cells do not (*J*). Horizontal scale bars (*A*, *D*, *G*, and *J*) represent 50 ms. Vertical scale bars in (*A*, *D*, *G*, and *J*) correspond to 0.5 nA (bars next to current pulses) and 20 mV (bars next to lowest voltage traces. In (*B*, *E*, *H*, and *K*), horizontal bars represent 1 ms and vertical bars 20 mV.

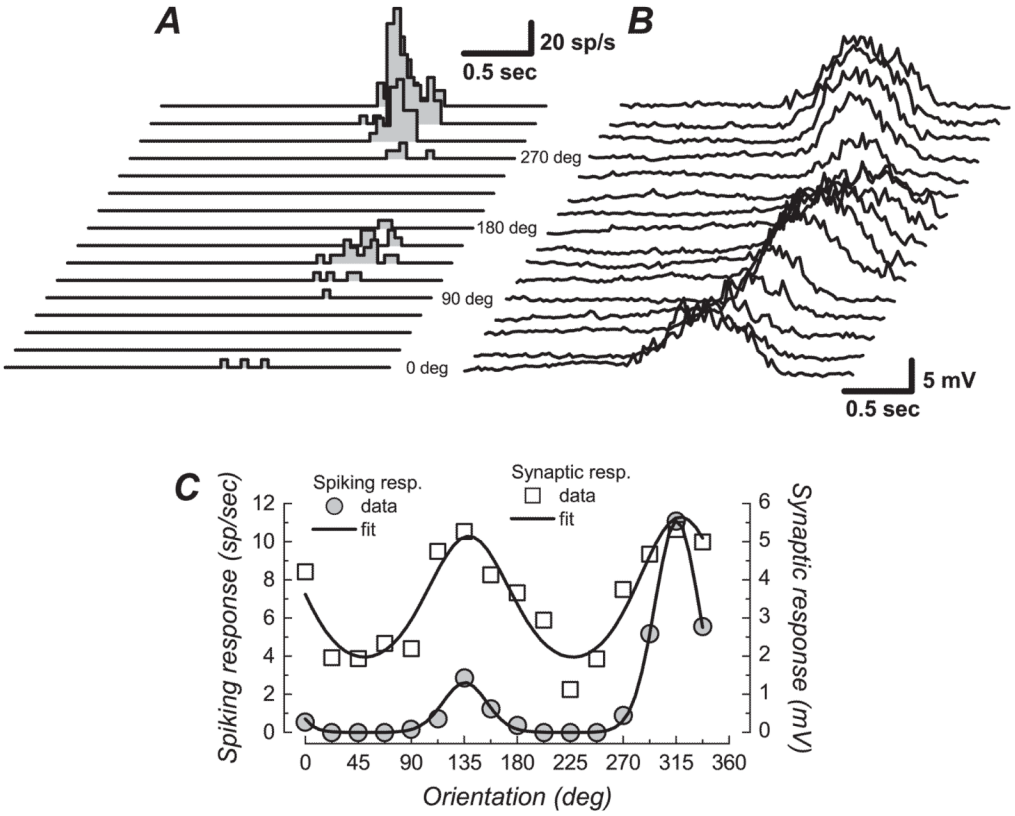

Figure 2.

Orientation tuning in a sharply tuned FS cell. (*A*) Spike response PSTHs for the 16 drifting bar stimuli (8 unique orientations and 2 motion directions). (*B*) Membrane potential average for the same stimuli. Resting membrane potential was −71 mV. (*C*) Fit of Von Mises equations to the spiking response (mean firing rate, scale on left) and to the synaptic response (mean membrane potential change, scale on right). The spiking response was sharply tuned for orientation (HWHH: 22 deg) and strongly direction selective (DnSI: 23%). The synaptic response was less orientation and direction selective (HWHH: 42 deg, DnSI: 91%). Note the presence of a significant depolarization for all the stimulus orientations (RURA: 26%).

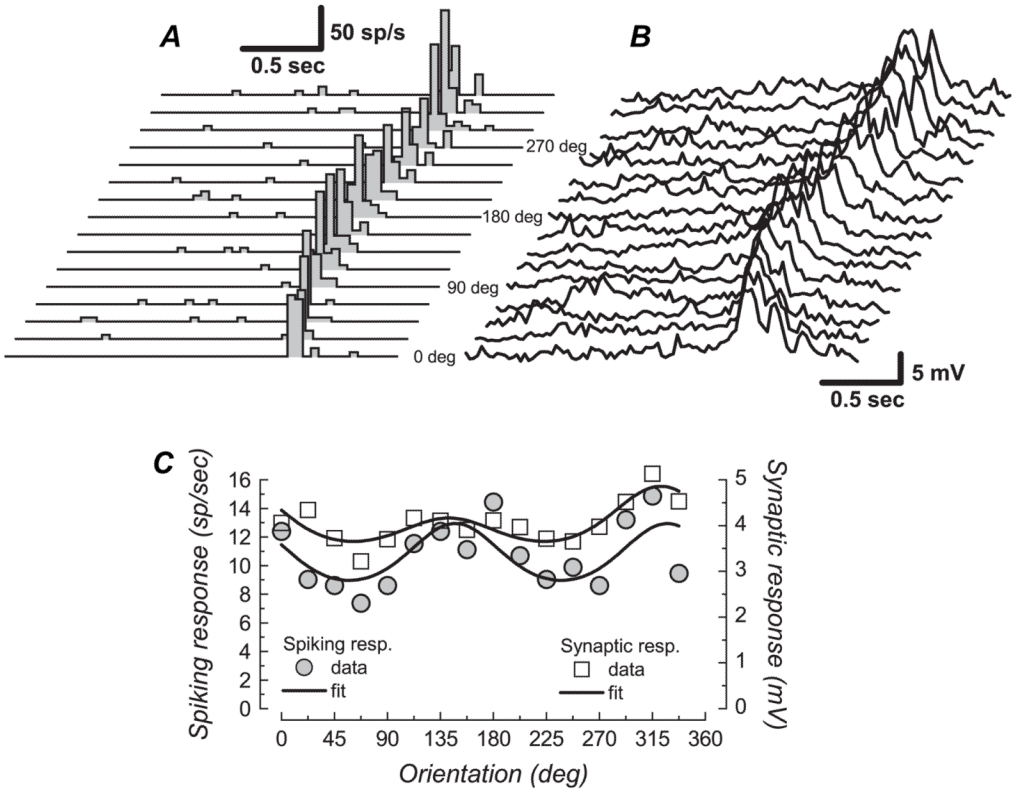

Figure 3.

Broadly tuned FS cell. (*A*) Spike response PSTH for the 16 directions. (*B*) Membrane potential average for the 16 directions. Resting membrane potential was −74 mV. (*C*) Von Mises fits to the spiking and synaptic responses. For the spiking response, the high RURA value (62%) and the large HWHH for the tuned response component (45 deg) indicate this cell was weakly orientation selective. The synaptic response was even less selective (RURA: 71%, HWHH: 47 deg).

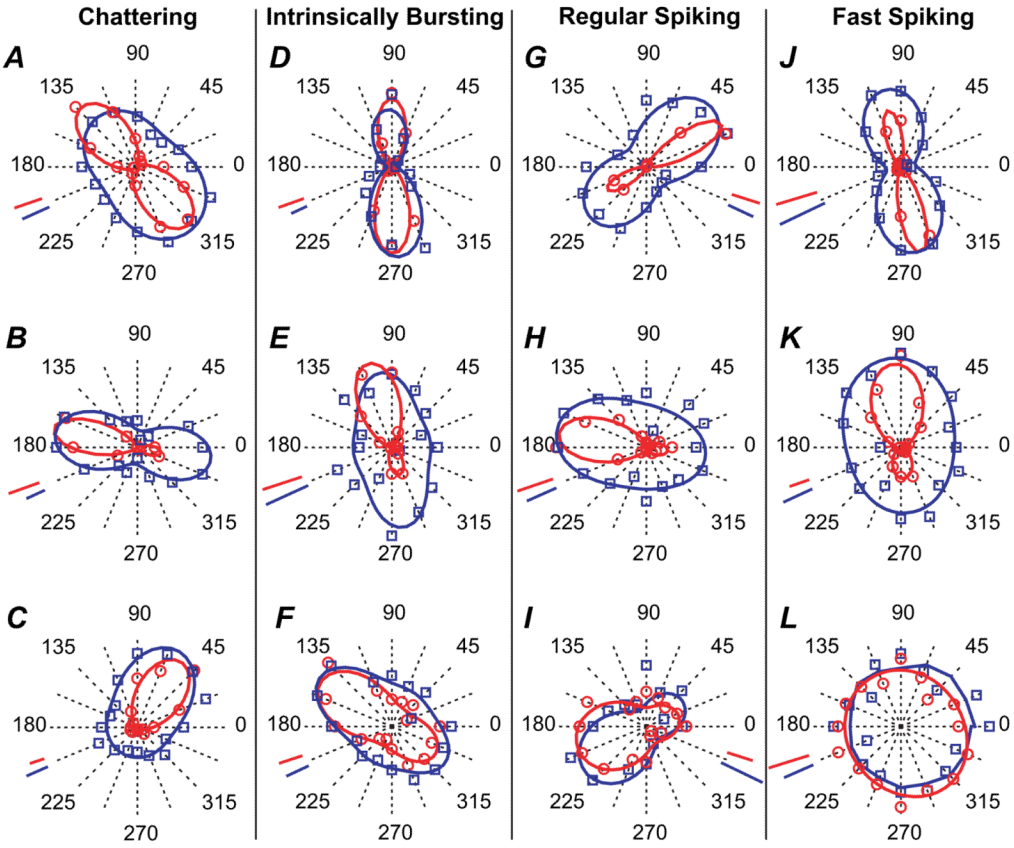

Figure 4.

Polar plots illustrating examples of orientation tuning curves for neurons belonging to the 4 electrophysiologically defined cell classes. The experimental data are displayed as data points, and the continuous lines represent the best fit to these data obtained with modified Von Mises' formula. Data and lines in red correspond to spiking responses and data and lines in blue to postsynaptic responses. (*A–C*) Orientation tuning in CH cells. (*D–F*) Orientation tuning in IB cells. (*G–I*) Orientation tuning in RS cells. (*J–L*) Additional examples of orientation tuning in FS cells. For the FS cell in (*L*), the postsynaptic data could not be fit and the line corresponds, for illustration purpose only, to a smoothed (3 point average) version of the actual data. Scale bars in red represent 10 spikes/s except in (*G*) (3 spikes/s), (*I*) (5 spikes/s), (*J*) (5 spikes/s), and (*K*) (20 spikes/s). Scale bars in blue represent 2 mV except in (*K*) (1 mV) and (*L*) (1 mV).

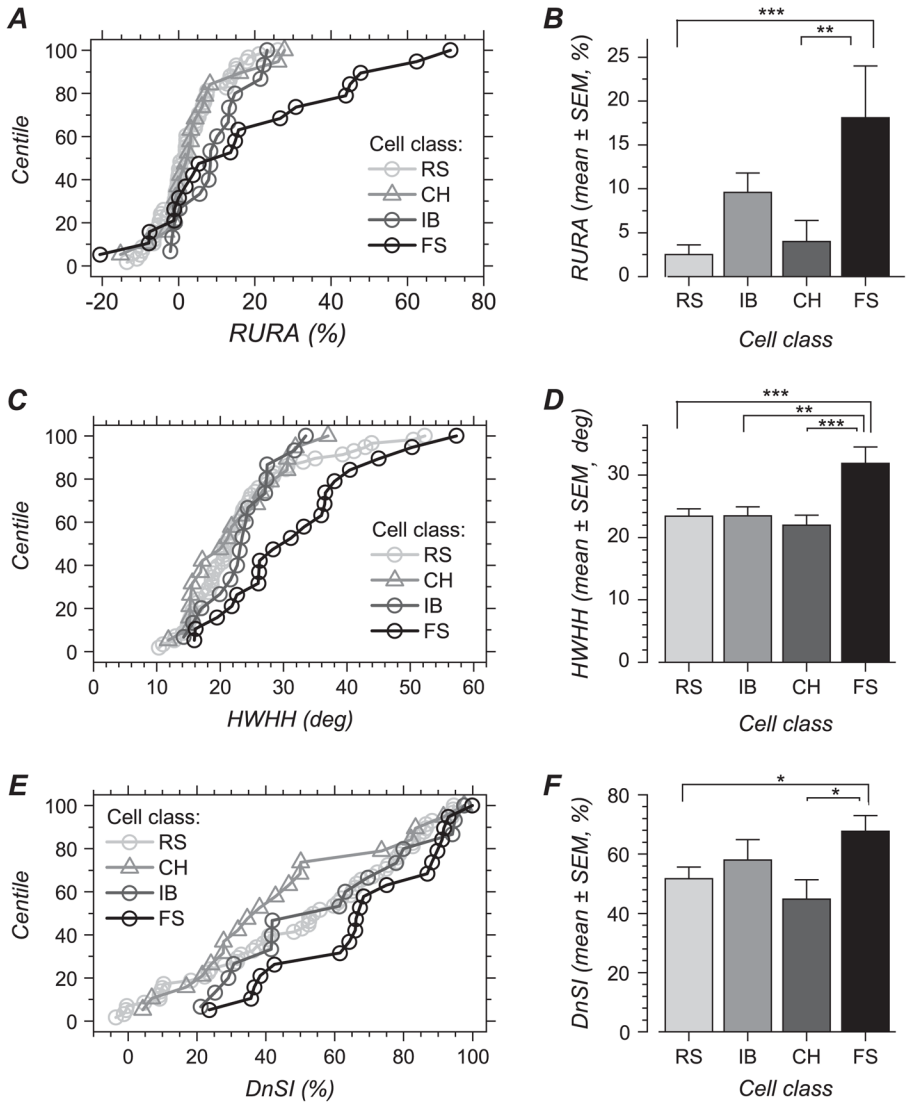

Figure 5.

Orientation and direction selectivity for spiking responses in electrophysiologically defined cell classes. (*A*) Cumulative distribution of RURA for each cell class. (*B*) Mean RURA for each cell class. (*C*) Cumulative distribution of orientation tuning HWHH for each cell class. (*D*) Mean HWHH for each cell class. (*A*) Cumulative distribution of DnSI for each cell class. (*B*) Mean DnSI for each cell class. Bars in (*B*, *D*, and *F*) represent one standard error of the mean. Significant differences between cell classes are indicated by stars, and the number of stars represents 3 significance level: ***, $P < 0.001$; **, $0.001 < P < 0.01$; *, $0.01 < P < 0.05$.

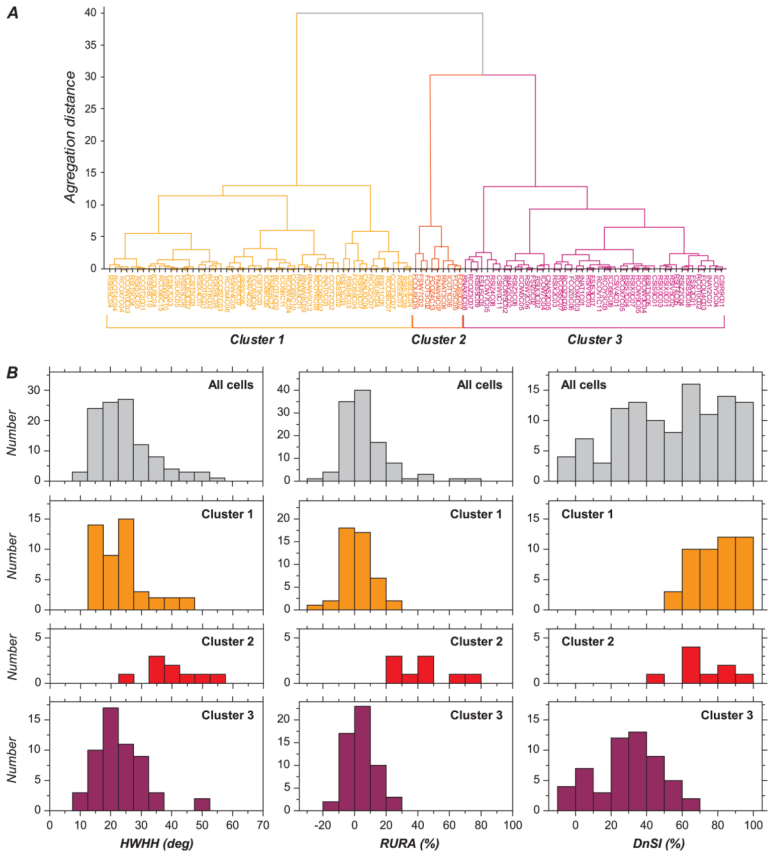

Figure 6.

Cluster analysis based segregation of 3 functional cell classes. (*A*) Hierarchical tree summarizing segregation of cells on the basis of the 3 variables used for quantification of orientation and direction selectivity. Main bifurcation at relatively large aggregation distances (distances ~40 and 30) leads to 3 well-isolated groups, labeled as cluster 1, cluster 2, and cluster 3. (*B*) Distribution histograms of HWHH (left), RURA (middle), and DnSI (right) for all the cells together and for each of the 3 clusters. Distributions for clusters 1, 2, and 3 are presented on the second, third, and fourth rows, respectively. For purpose of comparison, distribution for all the cells together is shown on the first row. Cluster 2 is different from clusters 1 and 3 in that it contains cells with larger HWHH and larger RURA. Cluster 2 appears to concentrate most of the cells that produced the skew in the total population histograms for RURA and HWHH. Cluster 3 is distinct from clusters 1 and 2 in that it contains cells that are more direction selective. This corresponds to the first mode in the distribution of DnSI when considering all of the cells together.

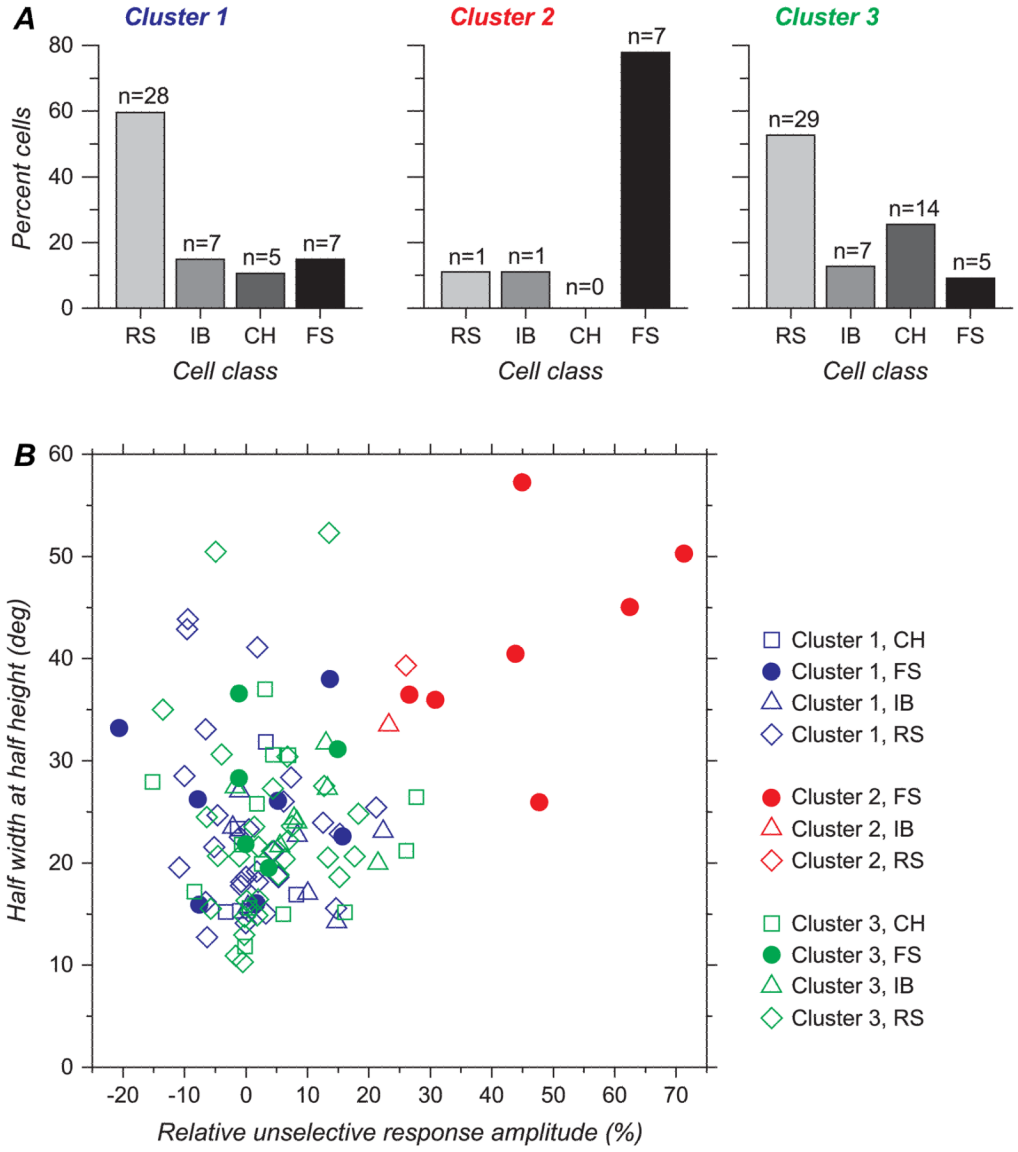

Figure 7.

(*A*) Proportion of each cell type in the 3 groups revealed by cluster analysis. Proportion of FS cells is much higher, and reciprocally, proportion of CH, RS, and IB cells much lower, in cluster 2 compared with clusters 1 and 3. (*B*) Scatter diagram representing HWHH versus RURA. Cluster 2 concentrates most of the cells with high values of HWHH together with high values of RURA. The 2 non-FS cells appear near the margin of clouds of dots representing cluster 2.

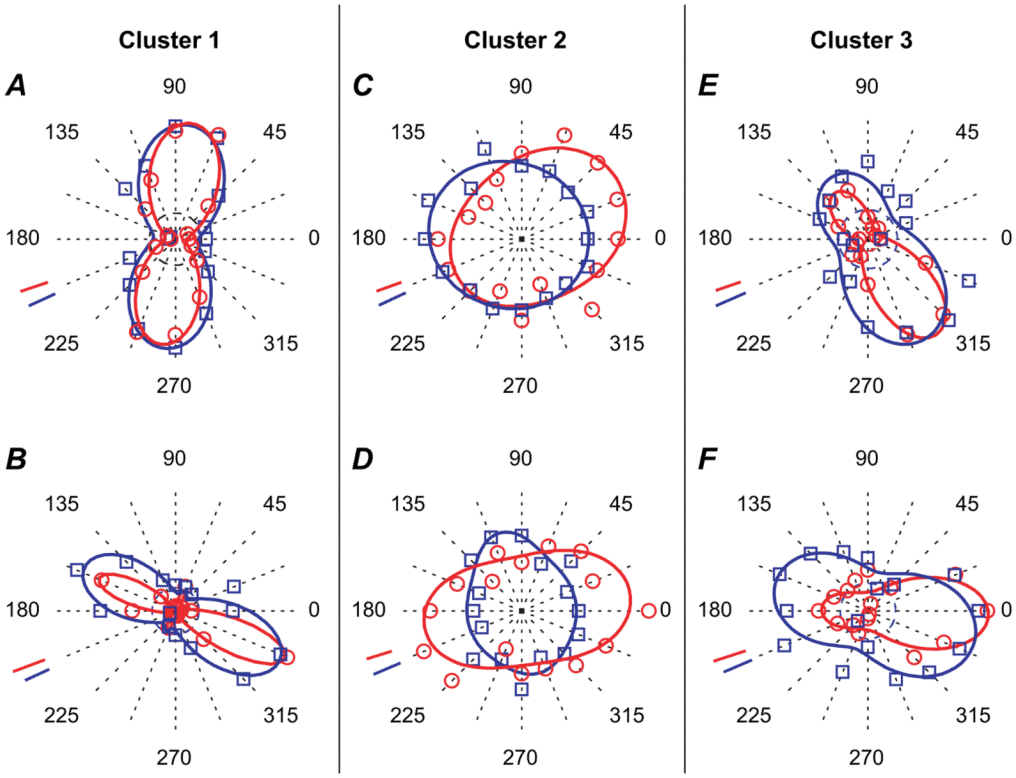

Figure 8.

Polar plots illustrating additional examples of orientation tuning curves for FS cells belonging to the 3 functionally defined clusters. The experimental data are displayed as data points, and the continuous lines represent the best fit to these data obtained with modified Von Mises' formula. Data and lines in red correspond to spiking responses and data and lines in blue to postsynaptic responses. (*A*, *B*) FS cells of cluster 1. Cluster 1 corresponds to cells that are orientation selective but not direction selective. (*C*, *D*) FS cells of cluster 2. Cells belonging to cluster 2 appear broadly tuned for orientation and direction. (*E*, *F*) FS cells of cluster 3. Cluster 3 contains cells that show both orientation and direction selectivity. Scale bars in red represent 20 spikes/s in (*A*), 5 spikes/s in (*B*), 5 spikes/s in (*C*), 1 spikes/s in (*D*), 2 spikes/s in (*E*), and 5 spikes/s in (*F*). Scale bars in blue represent 2 mV except in (*A*, *E*, and *F*) and 1 mV in (*B*, *C*, and *D*).

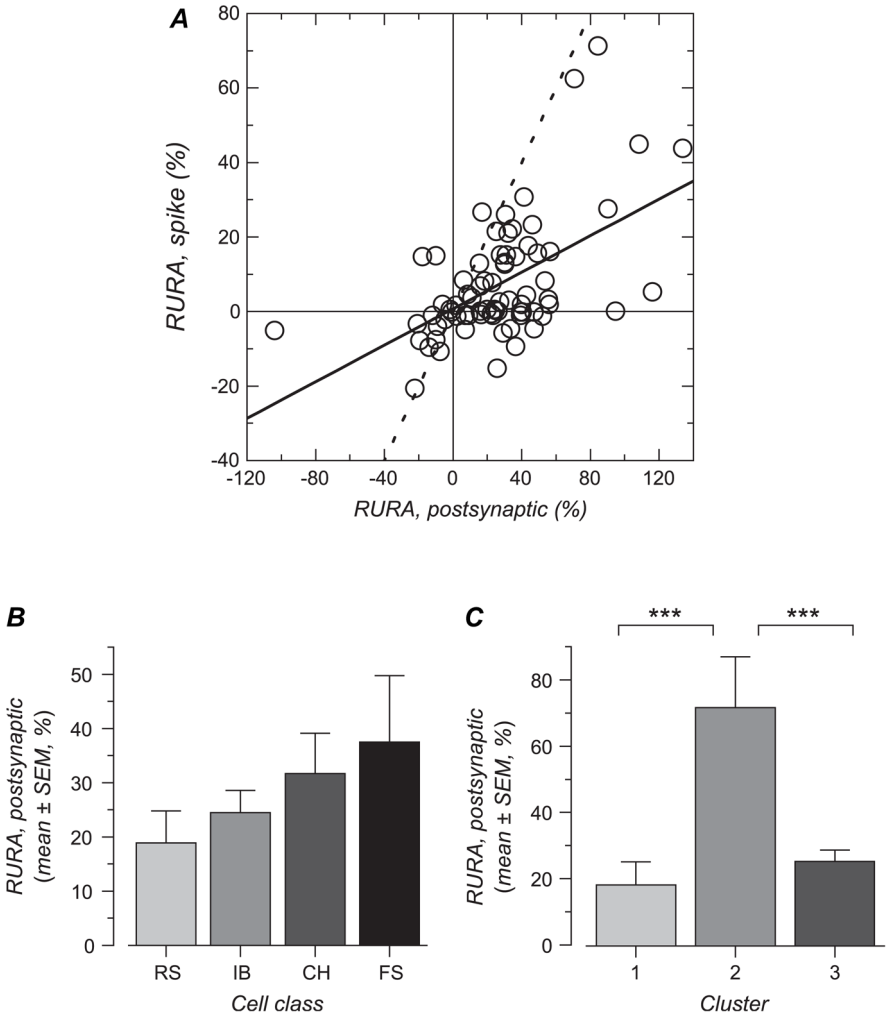

Figure 9.

Relative amplitude of the unselective response in the postsynaptic response and its relationship with relative amplitude of the unselective response in the spiking response. (*A*) RURA for spiking responses is plotted against RURA for postsynaptic responses for the whole population. The 2 variables are significantly correlated. The result of the linear regression analysis is shown by the solid line. For comparison, the dashed line shows a line of slope one. (*B*) Mean and standard error of mean (SEM) values for RURA calculated for the membrane potential response for each of the 4 electrophysiologically defined cell classes. Cell classes did not differ significantly. (*C*) Mean and SEM of RURA for each of the 3 clusters defined by orientation and direction selectivity. RURA was significantly larger for cells in cluster 2 compared with cells in clusters 1 and 3 (***, $P < 0.001$).

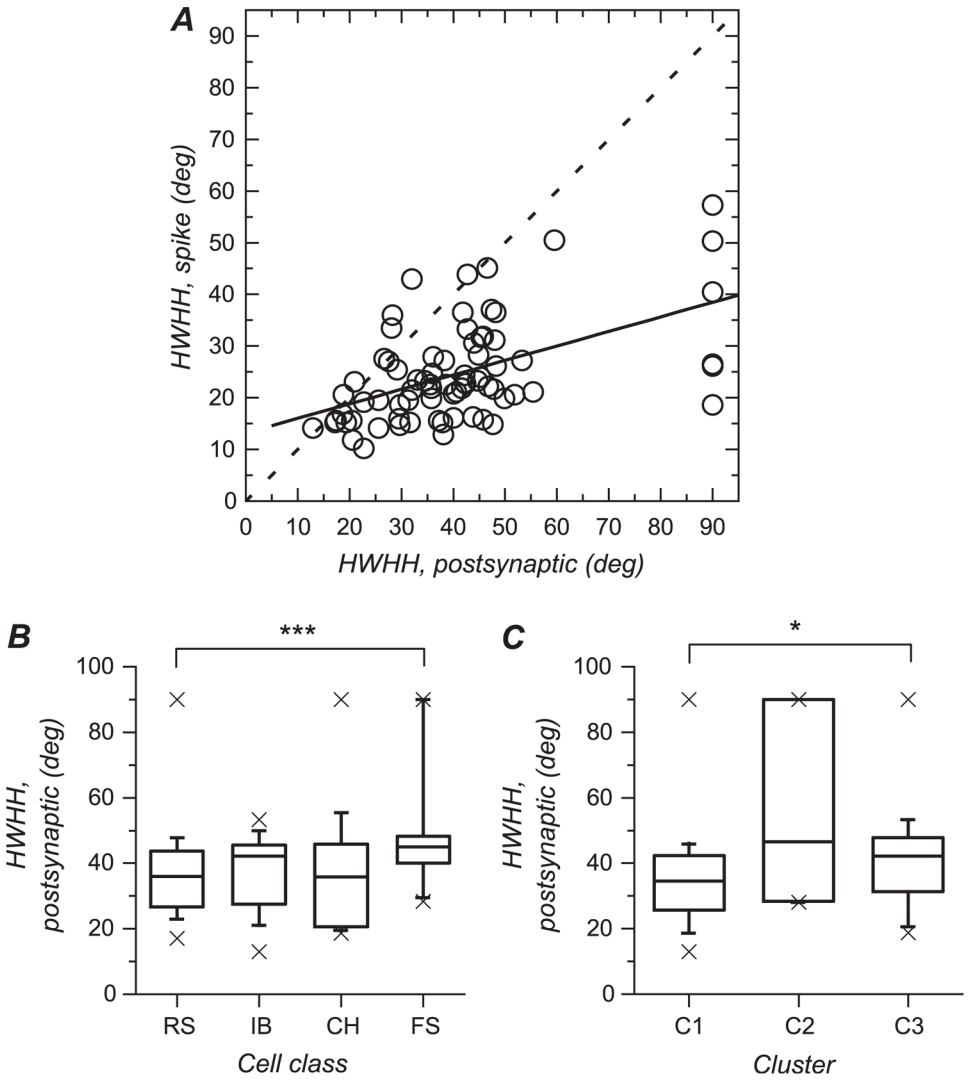

Figure 10.

HWHH of orientation tuning curves calculated for postsynaptic responses and relationship with spiking responses. (*A*) HWHH for spiking response plotted against HWHH for postsynaptic response. The 2 variables are significantly correlated. The regression line is represented by the solid line. The dashed line shows a line of slope one. Comparing the 2 lines also shows that HWHH for spike responses are quite systematically lower than HWHH for membrane potential responses. (*B*) Box plot representation summarizing HWHH for responses at the membrane potential level for each of the 4 electrophysiologically defined cell classes. The box delimits the 50% of the sample centered on the median, which is represented by the horizontal line within the box. Vertical lines and caps delimit the 10–90% centiles range. Crosses represent largest and smallest values. HWHH was significantly larger in FS cells compared with RS cells (***, $P < 0.001$). (*C*) Box plot for HWHH for each of the 3 clusters defined by orientation and direction selectivity. HWHH is significantly larger in cluster 3 compared with cluster 1 (*, $0.01 < P < 0.05$).

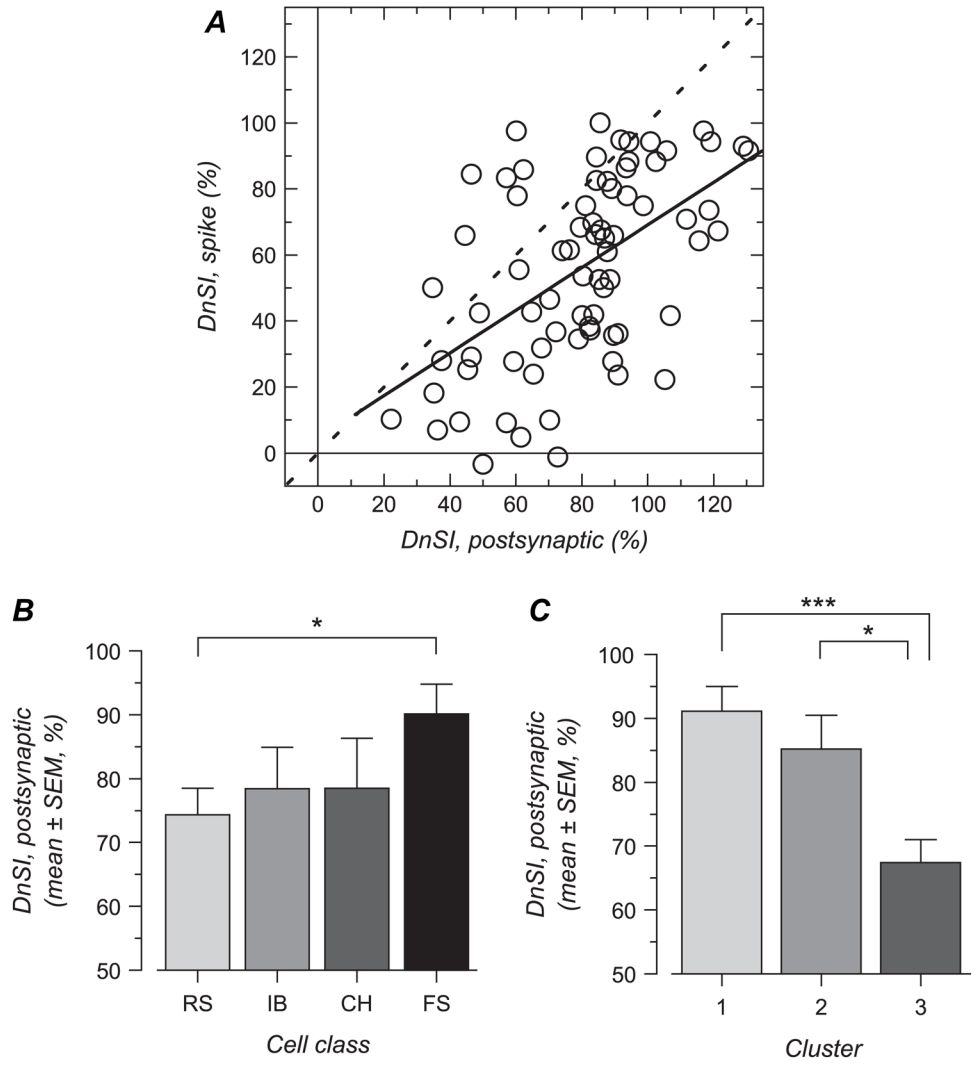

Figure 11.

Direction selectivity for postsynaptic responses and relationship with spiking responses. (*A*) When considering the whole population, DnSI for spiking response is significantly correlated with DnSI for synaptic responses. The result of the linear regression analysis is shown by the solid line. For comparison, the dashed line shows a line of slope one. (*B*) Mean and standard error of mean (SEM) values for DnSI calculated for the membrane potential response for each of the 4 electrophysiologically defined cell classes. RS and FS cells showed a significant difference (*, $0.01 < P < 0.05$). (*C*) Mean and SEM of DnSI shown for each of the 3 functionally defined clusters. Synaptic responses for cells in cluster 3 are more orientation selective (lower DnSI) than cells in clusters 2 and 1 (*, $0.01 < P < 0.05$; ***, $P < 0.001$).

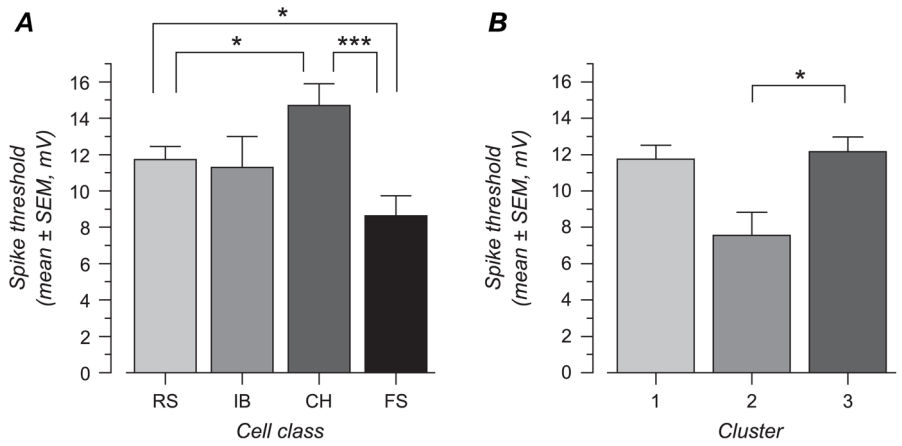

Figure 12.

Spike threshold varies between cell types and functionally defined clusters. (*A*) Spike threshold in electrophysiologically defined cell type. The lowest average spike threshold was found in FS and the highest in CH cells, with RS and IB cells occupying intermediate range. Differences were significant between FS and CH cells, between FS and RS cells, and between RS and CH cells. (*B*) Spike threshold for cells in cluster 2 is significantly lower than spike threshold in cluster 3. Stars indicate significance level: *, $0.01 < P < 0.05$; ***, $P < 0.001$.

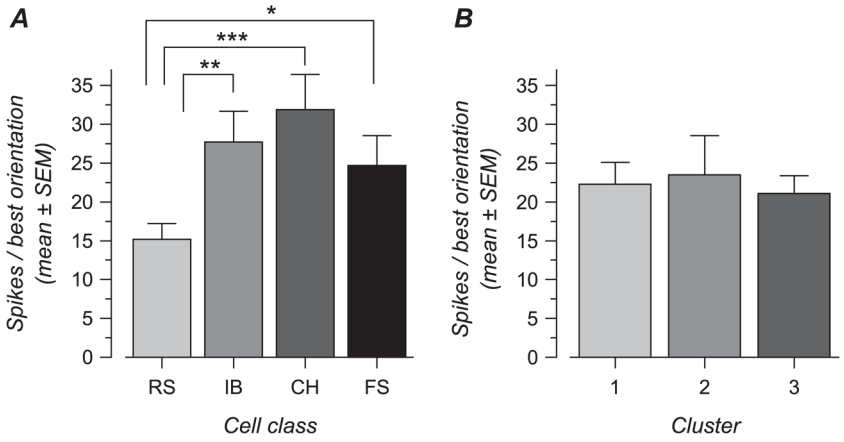

Figure 13.

Number of spikes induced by the preferred stimulus orientation. (*A*) RS cells show maximal firing rate that are lower than those obtained in other cell classes. (*B*) The number of spikes elicited by the optimal stimulus does not differ between functionally defined clusters.

Table 1

Orientation and direction selectivity in electrophysiological cell classes, spiking responses

	RS (*n* = 58)	IB (*n* = 15)	CH (*n* = 19)	FS (*n* = 19)
HWHH (deg)	23.4 ± 9.2	23.5 ± 5.5	22.0 ± 7.2	31.9 ± 11.3
RURA (%)	2.5 ± 8.5	9.6 ± 8.6	4.0 ± 10.3	18.1 ± 25.7
DnSI (%)	51.7 ± 29.8	58.0 ± 26.9	44.8 ± 28.4	67.7 ± 23.1

Note: Values are mean ± SD.

Table 2

Number of complex and simple RFs for each of the electrophysiologically defined cell class

	Simple	Complex
RS	32 (60.4%)	21 (39.6%)
IB	1 (10%)	9 (90%)
CH	9 (52.9%)	8 (47.1%)
FS	6 (35.3%)	11 (64.7%)
Total	48 (49.5%)	49 (50.5%)

Note: Numbers in parenthesis represent percentages of simple or complex cells within each electrophysiological cell class.

Table 3

Orientation and direction selectivity in the 3 functional clusters defined by orientation and direction selectivity indices, spiking responses

	Cluster 1 (*n* = 47)	Cluster 2 (*n* = 9)	Cluster 3 (*n* = 55)
HWHH (deg)	22.8 ± 7.7	40.5 ± 9.3	23.6 ± 8.4
RURA (%)	1.8 ± 8.9	41.9 ± 16.9	4.6 ± 8.8
DnSI (%)	79.0 ± 12.7	72.0 ± 18.0	29.9 ± 17.3

Note: Values are mean ± SD.

Table 4

Orientation and direction selectivity in electrophysiological cell classes, synaptic responses

	RS (*n* = 31)	**IB (*n* = 12)**	**CH (*n* = 14)**	**FS (*n* = 17)**
HWHH (deg)	35.9 ± 12.6	42.3 ± 17.8	36.0 ± 25.3	45.0 ± 19
RURA (%)	18.9 ± 32.9	24.5 ± 14.4	31.7 ± 27.6	37.5 ± 50.2
DnSI (%)	74.3 ± 23.5	78.4 ± 22.6	78.5 ± 29.0	90.1 ± 19.3

Note: Values for HWHH correspond to the median ± interquartile. Values for RURA and DnSI are mean ± SD.

Table 5

Orientation and direction selectivity in the 3 clusters defined by orientation and direction selectivity indices, synaptic responses

	Cluster 1 (*n* = 32)	**Cluster 2 (*n* = 7)**	**Cluster 3 (*n* = 35)**
HWHH (deg)	35.1 ± 15.9	46.6 ± 58.3	42.1 ± 15.3
RURA (%)	18.1 ± 7.0	71.6 ± 15.4	25.2 ± 3.5
DnSI (%)	91.1 ± 22.3	85.2 ± 14.0	67.4 ± 21.4

Note: Values for HWHH correspond to the median ± interquartile. Values for RURA and DnSI are mean ± SD.